IOWA STATE UNIVERSITY
Digital Repository

2007

Description of a superconducting transmission line having a weak link Josephson junction architecture

Norman E. Anderson

Iowa State University

Recommended Citation

Description of a superconducting transmission line having a weak link Josephson junction architecture

by

Norman E. Anderson

A thesis submitted to the graduate faculty

in partial fulfillment of the requirements for the degree of

MASTER OF SCIENCE

Major: Electrical Engineering

Program of Study Committee:
Mani Mina, Co-Major Professor
Robert Weber, Co-Major Professor
Alex Travesset

Iowa State University

Ames, Iowa

2007

UMI Number: 1446139

UMI®

TABLE OF CONTENTS

iii

LIST OF FIGURES

ABSTRACT

A Josephson junction consists of two superconductors separated by a non-superconducting layer, typically an insulator that is thinner than the Josephson penetration depth. We will explore this structure using the magnetic vector potential to describe the electromagnetic fields of a superconducting transmission line having the characteristics of a weak link Josephson junction. However, we will first revisit the beginnings of the Josephson junction and the conventional formulation techniques used to describe the electromagnetism of layered superconducting structures and Josephson junctions. We will then formally derive the field equations, for a transverse magnetic to z (TM^z) mode, for a superconducting transmission line, and take an in depth look at what these electromagnetic field equations represent. We will then discuss the Sine-Gordon equation and its role in the description and solution of Josephson junctions. This equation governs the coupling between superconductors separated by an insulating barrier, and it is this coupling that Josephson predicted. We continue on this path by revisiting the same superconducting transmission line, but take into account tunneling through the barrier using the Josephson current in our solution method. Finally, we will investigate using the finite difference method in order to numerically solve for the electromagnetic fields in our superconducting transmission line.

CHAPTER 1. MOTIVATION AND OVERVIEW

Devices using a Josephson junction architecture attract much attention because of their high sensitivity and novel attributes. A few of the realized and theorized applications include antennas [Suzuki et al. (1994)], transmission lines [Pond et al. (1989)], quantum computing [Faoro et al. (2003)], and possibly most notably its use in the SQUID (Superconducting QUantum Interference Device) magnetometer [Clarke et al. (1975)]. It is this driving force that has led to volumes of work on Josephson junctions and similar devices in hopes of discovering a new application or improving on current applications. It is this motivation that has led to us revisiting the problem of describing the electromagnetic field equations of a superconducting transmission line.

Initially, it was our focus to solve for the electromagnetic fields of a Josephson junction straightaway. However, after much research into the details of Josephson junctions, developing a solution method for the general layered superconducting transmission line was a more logical first step. Utilizing different techniques to describe this system may lead to different closed form solutions, which is still an ongoing activity [Wu et al. (2002)]. The general community uses the traditional approach that we will outline in Chapter 2, so the question of choosing a gauge is not necessary. In contrast, we see this gauge as a freedom to possibly make solutions in more complex geometries simpler. In addition, a fresh viewpoint can sometimes lead to a new discovery or perhaps a new description of a phenomenon.

1.1 Motivation

Here the magnetic vector potential, **A** is used in order to solve for the propagating electromagnetic fields of a superconducting transmission line. The magnetic vector potential is a useful mathematical tool because both the electric and magnetic fields are gauge invariant; allowing a scalar transformation of **A** without affecting the electromagnetic fields. For complex problems, applying this transformation to **A** can simplify the mathematics necessary to find the electromagnetic equations. This is increasingly useful as the geometry of the Josephson junction structures become more and more complex. With the utilization of **A**, a gauge can be selected to obtain a mathematically simple form of **A** for the case being dealt with. As an example of this concept, **A** will be utilized to solve a relatively simple superconducting transmission line problem having planar geometry. In addition, the Sine-Gordon equation will be investigated to obtain a representation of the coupling, and a general indication of where the linear approximation begins to break down.   Finally, the AC Josephson effect will be considered in our solution method. Using the Josephson current, a solution technique using the finite difference method will be investigated.

1.1.1 Magnetic Vector Potential

We will use the magnetic vector potential to solve for the propagating electromagnetic field equations for a superconducting transmission line. The superconducting transmission line structure considered is that of two superconductors separated by an insulating region. In this case, the separation between superconductors is great enough that Josephson tunneling phenomena can be ignored. We assume a TM^z mode

of propagation and solve directly for the magnetic vector potential using the Helmholtz equation in the Coulomb gauge.

Since the magnetic and electric fields are gauge invariant we can select a gauge which is mathematically simple in order to solve for the magnetic vector potential. This gauge invariance is one of the benefits of this solution method when dealing with more complicated structures. In our example the structure is simple to show how the method is used. Using the calculated value of the magnetic vector potential, the electric and magnetic fields can be calculated quite simply using two separate formulas given at the end of this chapter. The utilization of the magnetic vector potential to solve for the electromagnetic fields in this structure is in tune with Josephson's original concepts for layered superconducting structures [Josephson (1964)], and yields similar results calculated in recent literature using other analytical techniques [Wu et al. (2002)].

1.1.2 Sine-Gordon Equation

The Sine-Gordon equation characterizes the phase across the barrier of a Josephson junction. In essence it contains information about the coupling between the superconductors. We will look at the non-stationary and stationary versions of this equation. The stationary version has long been used in problem solutions yielding acceptable results. However, we will solve both the stationary and non-stationary forms of this equation in order to determine where this approximation is accurate. Also, this exercise will show how modern mathematical software can solve complex problems, previously needing approximations, in a simple and compact graphical form.

In our solution to the Sine-Gordon equation we will use realistic numbers for the Josephson frequency and length. This will give us a more accurate representation of the time dependence of this solution, and therefore the time dependence of the coupling between superconductors. While it seems we are neglecting the length of the barrier between conductors in our analysis, we will discuss how this thickness is inherently coupled to the time dependence of the tunneling effect.

1.1.3 Solution Using the Josephson Current

The Sine-Gordon equation bridges the gap between two superconductors separated by an insulating region and two superconductors that are coupled through the insulating region. While our description is relying purely on classical electrodynamics with results obtained using quantum mechanics, the full description of a Josephson junction and related phenomena are governed by quantum mechanics. Under the initial conditions of our structure we will use the current density for the AC Josephson effect in order to solve for the field equations of a superconducting transmission line having a weak-link Josephson junction architecture. This formulation leads to a transcendental equation which is not readily solved using analytical techniques. In this case we will attempt a numerical solution to this problem, which will also allow for more complex geometries to be solved provided initial conditions are known. Still, the basic principles of using the Helmholtz equation with the magnetic vector potential will be invoked.

1.2 Electromagnetic Description

Throughout the introduction it was heavily expressed that the magnetic vector potential, **A** will be used in our solution techniques along with the Helmholtz equation to give us a classical description of a superconducting transmission line. The magnetic vector potential is defined by

$$\mathbf{B} = \nabla \times \mathbf{A}. \tag{1}$$

Where **B** is the magnetic flux density. This relation was born from the realization that if $\nabla \cdot \mathbf{B} = \mathbf{0}$ everywhere, then **B** must be the curl of some vector field [Jackson (1999)]. Remembering that the curl of the gradient of a scalar variable is zero, **A** can be transformed by such a quantity without affecting **B** as shown in equation (2).

$$\mathbf{A} \to \mathbf{A}' = \mathbf{A} + \bar{\nabla}\Lambda$$
$$\mathbf{B} = \nabla \times \mathbf{A}' = \nabla \times \left(\mathbf{A} + \bar{\nabla}\Lambda \right) = \nabla \times \mathbf{A} \tag{2}$$

This transformation of **A** is known as a gauge transformation, and the fact that **B** is unchanged under such a transformation of **A** makes **B** a gauge invariant field. This gauge invariance of **B,** makes **A** an extremely useful mathematical tool. The way in which we can use **A** is through the Helmholtz equation

$$\nabla^2 \mathbf{A} - \frac{1}{c^2}\frac{\partial^2 \mathbf{A}}{\partial t^2} = \mu \mathbf{J}. \tag{3}$$

This wave equation relates **A** to the current density, **J** of the structure under consideration. By knowing or constructing **J**, we can then determine **A** and the resulting electromagnetic fields. We have already seen how **B** can be determined from **A** using equation (1), but how is the electric field, **E** determined from **A**? Remembering way back now to the equations we dreamed about in our sleep, we see that Maxwell has given us what we need

$$\nabla \times \mathbf{E} = -\frac{\partial \mathbf{B}}{\partial \mathbf{t}}. \tag{4}$$

While this is a simple and beautiful relation, we can even simplify one step further using equation (1) to find

$$\mathbf{E} = -\frac{\partial \mathbf{A}}{\partial t}. \tag{5}$$

We now have our equations for the electromagnetic fields based on the magnetic vector potential.

Up to this point we have neglected a very important quantity, the electric scalar potential, Φ and we will continue to do so throughout our solution method by neglecting any free static charge. However, as we will discuss near the end, this quantity may be a necessary component to consider in a layered structure with external bias, and could be the subject of future work. In addition we note that our description is utilizing classical electrodynamics and not a fully quantum mechanical description. While certain quantities, such as the Josephson current, have been derived quantum mechanically, our solution will not have the same quantization.

Armed now with equations (1), (3), and (5) we have the foundation necessary to begin our solution method for a superconducting transmission line without coupling. Before we dive into our solution method, we first briefly recapitulate Josephson's initial work and review two of the conventional methods for calculating the electromagnetic properties of a layered superconducting structure. We will then show how our method of using **A** can be used in a similar manner for probing the electromagnetic properties of layered superconducting structures, and may even have some benefits over the traditional approaches.

CHAPTER 2. A BRIEF HISTORY AND REVIEW

Even before the advent of Josephson's initial paper "Possible new effects in superconductive tunneling" [Josephson (1962)], much interest and excitement existed over the structure that would later be known by Josephson's name. Scientists such as P.W. Anderson, A. B. Pippard (Josephson's advisor), and J. C. Swihart among others were intently trying to unravel the mysteries of coupling and electromagnetic propagation in superconducting devices of different architectures in hopes of discovering a novel application, some new and exotic physics, or a physical realization of a past theory.

While none of this flurry of work would be possible without the discovery of superconductivity by Heike Kamerlingh Onnes in 1911 when he observed the disappearance of resistance in mercury at liquid Helium temperatures, the interpretation of superconductivity as a quantum phenomena by Fritz London in 1935, the modification of London's theory by Ginzburg and Landau in 1950 giving us an equation by their names, or the microscopic (BCS) theory of superconductivity developed by Bardeen, Cooper, and Schrieffer in 1957; we will not discuss these events here. The interested reader is pointed in the direction of books such as "Superconductivity" [Ginzburg and Andryushin (2004)], whose first chapter on the discovery of superconductivity is found free on the publisher's website. We continue our discussion on the history of layered superconducting structures by briefly looking at the work preceding Josephson, the influences on Josephson's work, and finally on two prominent results of Josephson's efforts.

2.1 Beginnings of the Josephson Junction

Long before Josephson was his student, Alfred Brian Pippard was considering the various differences between superconductors and normal metals. Most notably would be his series of three papers in 1947 in which he discussed surface and penetration effects in superconductors [Pippard (1947)]. It was in this series of papers that Pippard discussed that a wave in a superconducting transmission line would be slowed down because of the penetration of the magnetic field into the superconductor. It was this one point in Pippard's series of papers that struck D. R. Young in 1960, and led him to believe that this phenomenon may be used to measure the penetration depth of a superconductor. In turn, one of Young's collaborators was intrigued by this idea and attempted an electromagnetic field solution for a layered superconducting transmission line [Swihart (1960)], similar to the one we will encounter later. It was this work by Swihart as well as that by Wu et al. that motivated us to develop a solution method before considering the problem in full.

In his paper, Swihart considers two superconductors separated by a lossy dielectric and uses Maxwell's equations to calculate attenuation, wave velocity, and the electric and magnetic fields propagating through the structure. While Swihart's inspiration, initially beginning with Pippard, led him to look at electromagnetic propagation in layered superconducting structures, Pippard's own student, Josephson, found inspiration to look at layered superconducting structures from a different source.

2.1.1 Josephson's Research

As Josephson describes in his paper "Discovery of Tunneling Supercurrents" [Josephson (1974)], it was in a lecture given by visiting professor P.W. Anderson on how the

ground state of a superconductor breaks the symmetry of the pseudospin Hamiltonian that Josephson first started to conjure up his ideas that led to his discovery of tunneling through barriers. This lecture on symmetry breaking fascinated Josephson and led him to wonder whether it could be observed experimentally. It was this question and the support and suggestions of Anderson and Pippard that led to Josephson's calculation of the tunneling supercurrents between a pair of superconductors separated by an insulating region. While the explanation of the tunneling effect in Josephson's first paper [Josephson (1962)] was not correct, the work inspired because of this paper, by Josephson and others, soon described this curious event. Today, in most solid state physics books, a chapter can be found on Josephson tunneling describing both the DC and AC Josephson effects.

2.1.2 The DC Josephson Effect

The DC Josephson effect is the phenomenon of a dc current flowing across the insulating region separating two superconductors in the absence of an applied electric or magnetic field [Kittel (1996)]. If we let φ_1 be the wave function for one superconductor and φ_2 be the wave function for the other superconductor, then using the time-dependent Schrödinger equation we find

$$i\frac{\partial \varphi_1}{\partial t} = T\varphi_2 \text{ and } i\frac{\partial \varphi_2}{\partial t} = T\varphi_1. \qquad (6)$$

In this equation T has the units of frequency and is a measure of the "leakage" across the boundary from each wave function. In the case of a very thick insulator the value of T would be zero and there would be no tunneling across the barrier. If we assume superconductors

with wave functions of the form $\varphi \sim \sqrt{n}e^{i\theta}$, we can substitute this function into equation (6) to find

$$i\frac{\partial \varphi_1}{\partial t} = i\left(\frac{e^{i\theta_1}}{2\sqrt{n_1}}\frac{\partial n_1}{\partial t} + i\sqrt{n_1}e^{i\theta_1}\frac{\partial \theta_1}{\partial t}\right) = T\varphi_2$$

$$i\frac{\partial \varphi_2}{\partial t} = i\left(\frac{e^{i\theta_2}}{2\sqrt{n_2}}\frac{\partial n_2}{\partial t} + i\sqrt{n_2}e^{i\theta_2}\frac{\partial \theta_2}{\partial t}\right) = T\varphi_1. \tag{7}$$

Multiplying the top equation of (7) by $\sqrt{n_1}e^{-i\theta_1}$ and the bottom equation of (7) by $\sqrt{n_2}e^{-i\theta_2}$

$$i\left(\frac{1}{2}\frac{\partial n_1}{\partial t} + in_1\frac{\partial \theta_1}{\partial t}\right) = T\sqrt{n_2 n_1}\left(\cos\left(\theta_2 - \theta_1\right) + i\sin\left(\theta_2 - \theta_1\right)\right)$$

$$i\left(\frac{1}{2}\frac{\partial n_2}{\partial t} + in_2\frac{\partial \theta_2}{\partial t}\right) = T\sqrt{n_1 n_2}\left(\cos\left(\theta_2 - \theta_1\right) - i\sin\left(\theta_2 - \theta_1\right)\right). \tag{8}$$

Equating real and imaginary components for the top and bottom equations of (8) we find

$$\frac{\partial n_1}{\partial t} = 2T\sqrt{n_2 n_1}\sin\left(\theta_2 - \theta_1\right) \text{ and } \frac{\partial \theta_1}{\partial t} = -T\sqrt{\frac{n_2}{n_1}}\cos\left(\theta_2 - \theta_1\right)$$

$$\frac{\partial n_2}{\partial t} = -2T\sqrt{n_1 n_2}\sin\left(\theta_2 - \theta_1\right) \text{ and } \frac{\partial \theta_2}{\partial t} = -T\sqrt{\frac{n_1}{n_2}}\cos\left(\theta_2 - \theta_1\right). \tag{9}$$

If now we assume identical superconductors i.e., $n_1 \cong n_2$, we find the following relation for the phase difference

$$\frac{\partial \theta_2}{\partial t} = \frac{\partial \theta_1}{\partial t} \Rightarrow \frac{\partial}{\partial t}\left(\theta_2 - \theta_1\right) = 0. \tag{10}$$

From this result, we see there is no time rate of change for the phase across the boundary under zero applied bias, as we would expect. After seeing this result we might expect a time dependent phase difference if we were to apply a DC bias across the junction, but we will have to wait until the next section to find out. It is defined that the current flow from

superconductor 1 to superconductor 2 is proportional to $\partial n_2 / \partial t$ [Kittel (1996)] yielding a current across the junction having the form

$$J = J_0 \sin\left(\theta_2 - \theta_1\right). \tag{11}$$

It is apparent from this equation that J_0 is dependent on the "leakage" T, and a maximum and minimum current occur when the superconductor wave functions are 90° and 0° out of phase.

2.1.3 The AC Josephson Effect

The AC Josephson effect occurs when the Josephson junction has an applied DC bias V. Under this condition, a radio frequency current oscillates across the barrier. This effect has led to the successful development of the SQUID magnetometer, and will be the topic of further discussion in later sections. In order to calculate the current produced by this phenomenon, we begin by considering an electron pair that experiences a potential difference of qV when passing through the insulating region of the junction. Since the charge on a pair of electrons is -2e, the potential difference is then -2eV, and we can conclude that the potential energy at one superconductor is eV and at the other the potential energy is $-eV$.

Similarly to the method used to determine the current density for the DC Josephson effect, we begin by using the time-dependent Schrödinger equation which now takes the form

$$i\hbar \frac{\partial \varphi_1}{\partial t} = \hbar T \varphi_2 - eV \varphi_1 \text{ and } i\hbar \frac{\partial \varphi_2}{\partial t} = \hbar T \varphi_1 + eV \varphi_2. \tag{12}$$

Using the same form of the wave functions that we used previously we find the following equation in a similar manner

$$i\left(\frac{1}{2}\frac{\partial n_1}{\partial t}+in_1\frac{\partial \theta_1}{\partial t}\right)=T\sqrt{n_2 n_1}\left(\cos\left(\theta_2-\theta_1\right)+i\sin\left(\theta_2-\theta_1\right)\right)-eVn_1$$
$$i\left(\frac{1}{2}\frac{\partial n_2}{\partial t}+in_2\frac{\partial \theta_2}{\partial t}\right)=T\sqrt{n_1 n_2}\left(\cos\left(\theta_2-\theta_1\right)-i\sin\left(\theta_2-\theta_1\right)\right)+eVn_2.$$

(13)

Breaking the equation into real and imaginary parts again we find

$$\frac{\partial n_1}{\partial t}=2T\sqrt{n_2 n_1}\sin\left(\theta_2-\theta_1\right)\text{ and }\frac{\partial \theta_1}{\partial t}=\frac{eV}{\hbar}-T\sqrt{\frac{n_2}{n_1}}\cos\left(\theta_2-\theta_1\right)$$
$$\frac{\partial n_2}{\partial t}=-2T\sqrt{n_1 n_2}\sin\left(\theta_2-\theta_1\right)\text{ and }\frac{\partial \theta_2}{\partial t}=-\frac{eV}{\hbar}-T\sqrt{\frac{n_1}{n_2}}\cos\left(\theta_2-\theta_1\right).$$

(14)

We see that the relations for time rate of change of n_1 and n_2 are the same as what we have seen before in the calculation of the current density for the DC Josephson effect, however it is obvious that the derivative with respect to time of the phase difference across the junction will be different. Combining and simplifying the above equations, and again assuming identical superconductors we find the following result

$$\frac{\partial}{\partial t}\left(\theta_2-\theta_1\right)=\frac{-2eV}{\hbar}.$$

(15)

Now for the case of the Josephson junction under an applied DC bias, we see that there is indeed a time varying component of the phase. Integrating equation (15) with respect to time we find

$$\theta_2(t)-\theta_1(t)=\delta(t)=\delta(0)-\frac{2eVt}{\hbar}.$$

(16)

Substituting this result into the current density equation in the same fashion as before we find

$$J=J_0\sin\left(\delta(0)-\frac{2eVt}{\hbar}\right).$$

(17)

This is the AC Josephson effect, where J_0 is dependent on the "leakage" T. We will revisit this result later in our investigation of the electromagnetic description of a weak-link

Josephson junction transmission line. From equation (17) it is apparent that the current for this system oscillates with a frequency given by

$$\omega = 2\pi\upsilon = \frac{2eV}{\hbar}. \tag{18}$$

Using this equation for the frequency we note that the ratio of the frequency υ and the voltage is given by

$$\frac{\upsilon}{V} = 483.6 \frac{\text{MHz}}{\mu\text{V}}. \tag{19}$$

This tells us that as an electron pair crosses the Josephson junction barrier, a photon is either emitted or absorbed having an energy, $E = \hbar\omega = 2eV$. This result clearly shows the quantized nature of the energy states of the Josephson junction. Parker and others [Parker et al. (1967)] determined, and it is also clearly seen by the energy relation, that by measuring the voltage and frequency across the junction the value of $e/\hbar$ could be determined with great precision. Experimental evidence of this arises in a variety of situations. An example being the interaction between the AC Josephson current and the microwave signal that occurs under irradiation of a Josephson junction with microwaves. In this case, steps are seen in the V-I characteristic at voltages given by

$$V_n = \frac{nh}{2e}\upsilon. \tag{20}$$

Here n is an integer and υ is the frequency of the applied radiation. This phenomenon was first seen by Shapiro [Shapiro (1963)].

These are two extremely powerful and intriguing results discovered by Josephson, and research still continues to this day because of Josephson's curiosity during a lecture by P.W. Anderson.

2.2 Review of Conventional Solution Methods

In this section we review two of the basic solution methods used to determine the electromagnetic properties of a layered superconducting structure, and outline the solution methodology.   The two basic methods under consideration are the use of Maxwell's equations and the current density method. Both have been utilized in the study of Josephson junction research as well as other superconducting phenomena [Barone and Paternò (1982)].

We begin by looking at the fundamental approach of using Maxwell's equations to solve for the propagating fields in a Josephson junction, which we noted earlier was employed by Swihart in his investigation of propagation. Using this approach we will calculate the general form of the electromagnetic fields in terms of the phase difference across the boundary, and determine the dispersion relation of the system.

The next approach we will turn our attention to is the current density method. This method utilizes the two fluid model proposed by Gorter and Casimir [Gorter and Casimir (1934)], and uses Maxwell's equations as well to solve for the electromagnetic fields. Again, we will use this method to solve for the dispersion relation.

2.2.1 Traditional Approach

One of the earliest and simplest formulations of the propagating fields in a Josephson junction was completed using Maxwell's equations, and more precisely Ampere's and Faraday's laws, as depicted in Figure 1. This method was suggested by Josephson and calculated by many others since then with slight variations.

Traditional Approach
E is electric field intensity in V/m
H is magnetic field intensity
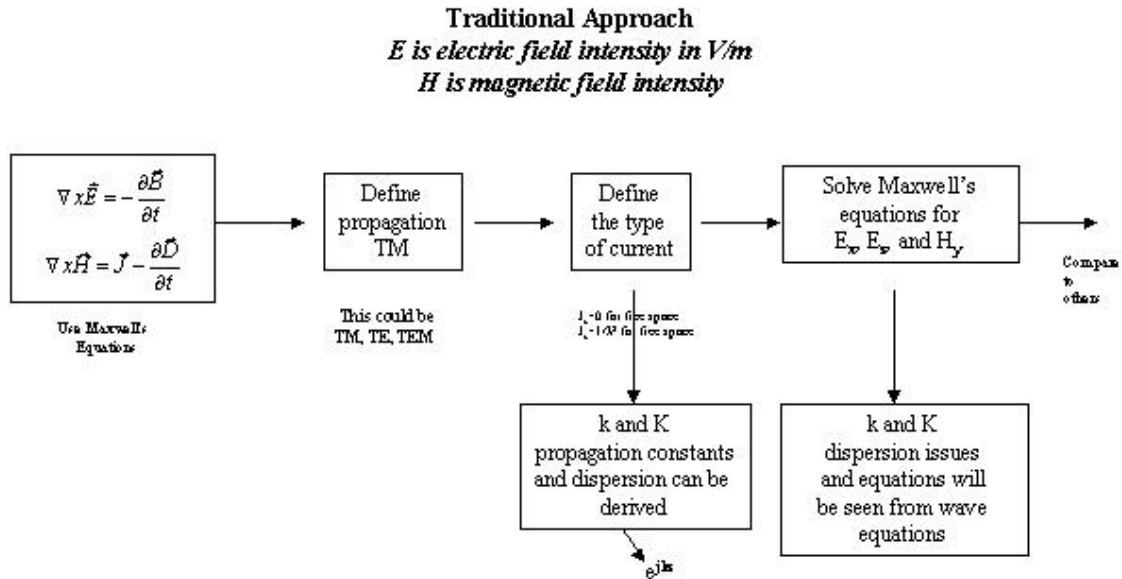
Figure 1. Traditional approach to solve for Josephson junction field equations.

For simplicity we assume that our Josephson junction consists of two identical superconductors and an insulator of thickness *D*. It is also assumed that the superconductors are much thicker than the penetration depth, *λ*. Figure 1 illustrates the junction of interest.
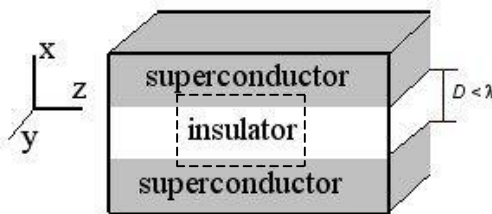
Figure 2. Superconducting layered structure.

In the above figure, the broken line will be chosen as a path of integration that extends deep enough into the superconductor so the fields are zero along the segments of *dz*

length parallel to the surface of the junction. The magnetic field is assumed to be nonzero in the *y*-direction and zero in the *x* and *z*-directions, and to penetrate into the superconductors a negligible distance. The electric field normal to the superconductors and the electric field normal to the superconductors is also assumed to penetrate a negligible distance. We then begin by using Faraday's law given by:

$$\vec{\nabla} \times \vec{E} = -\frac{\partial \vec{B}}{\partial t}. \tag{21}$$

Now, we can integrate this equation over the surface abcd.

$$\int_s \vec{\nabla} \times \vec{E} \cdot d\bar{s} = \int_s -\frac{\partial \vec{B}}{\partial t} \cdot d\bar{s} \tag{22}$$

The left hand side can then be rewritten using Stoke's law and the definition of a derivative with respect to *z*.

$$\int_s \vec{\nabla} \times \vec{E} \cdot d\bar{s} = \int_{a \to b \to c \to d \to a} \vec{E} \cdot d\bar{l} = \left\{ E_x(z+dz) - E_x(z) \right\} D = D \frac{\partial E_x}{\partial z} dz \tag{23}$$

Here, E_x is the electric field polarized in the *x*-direction inside the insulator. The right hand side is then evaluated giving us:

$$\int_s -\frac{\partial \vec{B}}{\partial t} \cdot d\bar{s} = -\frac{\partial B_y}{\partial t} \cdot (2\lambda + D)dz. \tag{24}$$

Again, B_y is the magnetic induction polarized in the *y*-direction inside the insulator. Equating (23) and (24) now gives rise to

$$\frac{\partial E_x}{\partial z} = -\frac{\partial B_y}{\partial t} \left(1 + \frac{2\lambda}{D} \right). \tag{25}$$

Operating on (25) with *d/dz* yields the following relation

$$\frac{\partial^2 E_x}{\partial z^2} = -\frac{\partial^2 B_y}{\partial z \partial t}\left(1+\frac{2\lambda}{D}\right). \tag{26}$$

If we now consider a similar surface but this time position it normal to the *z*-axis, it is easily shown that this results in

$$\frac{\partial^2 E_x}{\partial y^2} = \frac{\partial^2 B_y}{\partial y \partial t}\left(1+\frac{2\lambda}{D}\right). \tag{27}$$

This is similar to that seen for our original surface. Now using Maxwell's equation for Ampere's law we can derive another relation governing our Josephson junction.

$$\bar{\nabla}\times\vec{H} = \vec{J} + \varepsilon\frac{\partial \vec{E}}{\partial t} \tag{28}$$

Expanding this expression using the constitutive relation for *H* and *B*, and keeping only the *x*-components we have

$$\frac{1}{\mu}\left(\bar{\nabla}\times\vec{B}\right)_x = \frac{1}{\mu}\left(\frac{\partial B_z}{\partial y} - \frac{\partial B_y}{\partial z}\right) = J_x + \varepsilon\frac{\partial E_x}{\partial t}. \tag{29}$$

Now, taking the time derivative of this expression we obtain

$$\frac{1}{\mu}\left(\frac{\partial^2 B_z}{\partial t \partial y} - \frac{\partial^2 B_y}{\partial t \partial z}\right) = \frac{\partial J_x}{\partial t} + \varepsilon\frac{\partial^2 E_x}{\partial t^2}. \tag{30}$$

If we add (26) and (27) and multiply by $1/\mu$ we find that

$$\frac{1}{\mu}\left(\frac{\partial^2 B_z}{\partial t \partial y} - \frac{\partial^2 B_y}{\partial t \partial z}\right) = \frac{1}{\mu}\left(1+\frac{2\lambda}{D}\right)^{-1}\left(\frac{\partial^2 E_x}{\partial y^2} + \frac{\partial^2 E_x}{\partial z^2}\right). \tag{31}$$

The left hand side of (31) is then the same as the left hand side of (30). Now equating the right hand side of (30) with the right hand side of (31) and simplifying we have the following relation

$$\frac{\partial^2 E_x}{\partial y^2} + \frac{\partial^2 E_x}{\partial z^2} - \mu\varepsilon\left(1+\frac{2\lambda}{D}\right)\frac{\partial^2 E_x}{\partial t^2} = \left(1+\frac{2\lambda}{D}\right)\mu\frac{\partial J_x}{\partial t}. \tag{32}$$

We can then rewrite this expression by factoring out E_x to get

$$\left\{\frac{\partial^2}{\partial y^2} + \frac{\partial^2}{\partial z^2} - \mu\varepsilon\left(1+\frac{2\lambda}{D}\right)\frac{\partial^2}{\partial t^2}\right\}E_x = \left(1+\frac{2\lambda}{D}\right)\mu\frac{\partial J_x}{\partial t}. \tag{33}$$

We now define the phase velocity, v to be

$$v = \left\{\mu\varepsilon\left(1+\frac{2\lambda}{D}\right)\right\}^{-1/2}. \tag{34}$$

Rearranging this equation we find that

$$\mu\left(1+\frac{2\lambda}{D}\right) = \varepsilon v^2. \tag{35}$$

Substituting this result into equation (33) we now have

$$\left(\frac{\partial^2}{\partial y^2} + \frac{\partial^2}{\partial z^2} - \frac{1}{v^2}\frac{\partial^2}{\partial t^2}\right)E_x = \frac{1}{\varepsilon v^2}\frac{\partial J_x}{\partial t}. \tag{36}$$

It is seen that for the steady state where $\partial J_x/\partial t = 0$, equation (36) well describes a transverse electromagnetic (TEM) wave propagating between parallel plates with properties differing from a normal metal system. It is also observed that the phase velocity, v, is lowered by a factor equal to $(1+2\lambda/D)^{-1/2}$. To write equation (36) in terms of the phase change, φ across the junction we use

$$\frac{\partial\varphi}{\partial t} = \frac{2eV}{\hbar} = -\frac{2e}{\hbar}DE_x, \tag{37}$$

which we have derived in the previous section. Solving for E_x we find

$$E_x = -\frac{\hbar}{2eD}\frac{\partial\varphi}{\partial t}. \tag{38}$$

Substituting our equation for E_x into (36) we have

$$\left(\frac{\partial^2}{\partial y^2}+\frac{\partial^2}{\partial z^2}-\frac{1}{v^2}\frac{\partial^2}{\partial t^2}\right)\frac{\partial\varphi}{\partial t}=-\frac{2eD}{\hbar}\frac{1}{\varepsilon v^2}\frac{\partial J_x}{\partial t}. \tag{39}$$

Since $J_x=-J_c\sin\varphi$, where J_c is the superconducting critical current and φ is a

function of y and z, we introduce a new quantity λ_J such that

$$\lambda_J=\left\{\frac{\hbar}{2e\mu(D+2\lambda)J_c}\right\}^{1/2}. \tag{40}$$

This quantity is then commonly referred to as the Josephson penetration depth. Now

equation (39) can be written using λ_J as

$$\left(\frac{\partial^2}{\partial y^2}+\frac{\partial^2}{\partial z^2}-\frac{1}{v^2}\frac{\partial^2}{\partial t^2}\right)\frac{\partial\varphi}{\partial t}=\frac{1}{\lambda_J^2}\frac{\sin\varphi}{\partial t}. \tag{41}$$

Taking the time reference where $\varphi=0$ and integrating equation (41) with respect to

time at an arbitrary point (y,z) we have

$$\left(\frac{\partial^2}{\partial y^2}+\frac{\partial^2}{\partial z^2}-\frac{1}{v^2}\frac{\partial^2}{\partial t^2}\right)\varphi=\frac{\sin\varphi}{\lambda_J^2}. \tag{42}$$

This equation is then the equation Josephson obtained to describe the non-equilibrium

properties of barriers. It is more commonly referred to as the non-linear Sine-Gordon

equation. If the phase variations with time are small enough to be able to linearize (42) we

can then write

$$\varphi(y,z,t)=\varphi_0(y,z)+\varphi_1(y,z,t), \tag{43}$$

where $\varphi(y,z,t)$ is assumed to be small enough such that $\sin\varphi$ can be approximated by φ.

Substituting (43) into (42) and subtracting out the time-averaged quantities gives rise to

$$\left(\frac{\partial^2}{\partial y^2} + \frac{\partial^2}{\partial z^2} - \frac{1}{v^2}\frac{\partial^2}{\partial t^2} \right)\varphi_1 = \left(\frac{\cos\varphi_0}{\lambda_J^2} \right)\varphi_1 . \tag{44}$$

Since $\varphi(y, z, t)$ is assumed to be small, $\varphi_0 = 0$ and $\sin\varphi$ can be approximated by φ. With this assumption the solution of (44) is then given by

$$\varphi = e^{j(\vec{k}\cdot\vec{r} - \omega t)} . \tag{45}$$

Where in our present case $\vec{r}$ is in the plane of the junction. If φ is a solution of equation (44), then the we can derive the dispersion relation for the insulating barrier.

$$\frac{\partial^2\varphi}{\partial r^2} - \frac{1}{v^2}\frac{\partial^2\varphi}{\partial t^2} = \frac{\varphi}{\lambda_J^2}$$
$$-k^2\varphi + \frac{1}{v^2}\omega^2\varphi = \frac{\varphi}{\lambda_J^2} \tag{46}$$

Which simplifies to

$$\omega^2 = k^2 v^2 + \omega_J^2 . \tag{47}$$

Here ω_J is given by

$$\omega_J^2 = \left(\frac{v}{\lambda_J} \right)^2 . \tag{48}$$

It is obvious from this result that no propagating waves exist below ω_J.

2.2.2 Current Density Method

We begin this method using the same geometry seen in Figure 1 and for the TM^z mode. We also assume that due to the structure there is no current flow in the y-direction so $J_y = 0$. From these conditions we know $H_x = H_z = E_y = 0$ and H_y, E_x, and E_z are nonzero field components. According to the two-fluid model, the current density consists of two parts as shown in (49).

$$\mathbf{J} = \mathbf{J}_n + \mathbf{J}_s \tag{49}$$

Here, $\mathbf{J}_n$ is the normal part of the total current density defined by the classical skin effect

$$\mathbf{J}_n = \sigma \mathbf{E}, \tag{50}$$

also known as Ohm's law. $\mathbf{J}_s$ is the supercurrent density and must satisfy both London equations [London and London (1935)] which state

$$\nabla \times \mathbf{J}_s = -\frac{\mathbf{H}}{\lambda^2} \text{ and} \tag{51}$$

$$\mathbf{J}_s = \frac{\mathbf{E}}{j\omega\mu\lambda^2}. \tag{52}$$

We now set out to use these conditions in order to solve Maxwell's equations for the different regions of our superconducting structure. To do this we assume fields propagating in the z-direction having the form $\mathbf{E} = \mathbf{E}_0 e^{-j(k_z z - \omega t)}$. We can begin by using Maxwell's equation for Faraday's law given in phasor form

$$\nabla \times \mathbf{E} = -j\omega\mathbf{H}. \tag{53}$$

On expanding this equation we find the only nonzero resulting equation is then

$$-jk_z E_x - \frac{\partial E_z}{\partial x} = -j\omega\mu H_y. \tag{54}$$

We use Maxwell's equation for Ampere's law in phasor form to derive the other relations governing our structure.

$$\nabla \times \mathbf{H} = j\omega\varepsilon\mathbf{E} + \mathbf{J} \tag{55}$$

From this equation we find that there are two resulting nonzero equations

$$jk_z H_y = J_{nx} + J_{sx} + j\omega\varepsilon E_x \text{ and} \tag{56}$$

$$\frac{\partial H_y}{\partial x} = J_{nz} + J_{sz} + j\omega\varepsilon E_z. \tag{57}$$

Now, if we substitute into this equation the current density equations (50) and (52) we find that

$$jk_z H_y = \left(\sigma_x + \frac{1}{j\omega\mu\lambda^2} + j\omega\varepsilon \right) E_x \text{ and} \tag{58}$$

$$\frac{\partial H_y}{\partial x} = \left(\sigma_z + \frac{1}{j\omega\mu\lambda^2} + j\omega\varepsilon \right) E_z. \tag{59}$$

These two equations along with (54) make up the relations we will use to characterize our structure. Initially looking at the insulating layer we know that there is no current flow in this region so $\mathbf{J}_n = \mathbf{J}_s = 0$. We then see (56) reduces to

$$H_y = \frac{\omega\varepsilon E_x}{k_z}. \tag{60}$$

It is noted that equation (54) does not change form and (57) can be reduced to

$$\frac{\partial H_y}{\partial x} = j\omega\varepsilon E_z. \tag{61}$$

We can replace the left hand side of (61) with the result of (60) to obtain

$$\frac{\omega\varepsilon}{k_z} \frac{\partial E_x}{\partial x} = j\omega\varepsilon E_z. \tag{62}$$

Substituting (62) and (60) into (54) for fields E_z and H_y we see

$$-jk_z E_x + \frac{j}{k_z} \frac{\partial^2 E_x}{\partial x^2} = -\frac{j\omega^2\varepsilon\mu}{k_z} E_x. \tag{63}$$

Reducing this equation we finally find

$$\frac{\partial^2 E_x}{\partial x^2} = (k_z^2 - \omega^2\varepsilon\mu) E_x. \tag{64}$$

Assuming E_x has the following form inside the insulating region

$$E_x = \left(ae^{k_x x} + be^{-k_x x} \right) e^{j(k_z z - \omega t)},\tag{65}$$

we see that (64) then reduces to

$$k_x^2 = k_z^2 - \omega^2 \varepsilon \mu.\tag{66}$$

This is the dispersion relation for the insulating barrier of our structure. Now, we turn to the superconducting region where we have a nonzero supercurrent, $\mathbf{J}_s$. Due to the nonzero current density, equation (54) remains unchanged, and (58) and (59) lose their conductivity term. If we solve the modified version of (58) for H_y we find

$$H_y = \frac{\omega \varepsilon}{k_z} \left(1 - \frac{1}{\omega^2 \varepsilon \mu \lambda^2} \right) E_x.\tag{67}$$

Solving the modified version of (59) for E_z we obtain the result

$$E_z = \frac{1}{j\omega \varepsilon} \left(1 - \frac{1}{\omega^2 \varepsilon \mu \lambda^2} \right)^{-1} \frac{\partial H_y}{\partial x}.\tag{68}$$

If we replace H_y with the result from (67) we find

$$E_z = -\frac{j}{k_z} \frac{\partial E_x}{\partial x}.\tag{69}$$

Substituting the results of (67) and (69) into (53) we can determine the dispersion relation for the superconducting region of our structure

$$-jk_z E_x + \frac{j}{k_z} \frac{\partial^2 E_x}{\partial x^2} = -j\omega \mu \frac{\omega \varepsilon}{k_z} \left(1 - \frac{1}{\omega^2 \varepsilon \mu \lambda^2} \right) E_x$$

$$\frac{\partial^2 E_x}{\partial x^2} = \left(k_z^2 - \omega^2 \varepsilon \mu + \frac{1}{\lambda^2} \right) E_x.\tag{70}$$

Again assuming E_x is of the form given in (65), with $a = 0$ for the upper superconductor and $b = 0$ for the bottom superconductor to keep the electric field from diverging, we have

$$k_x^2 = k_z^2 - \omega^2 \varepsilon \mu + \frac{1}{\lambda^2}. \tag{71}$$

This is the dispersion relation for the superconducting region of our structure. We see that the only difference between this relation and the one for the insulating layer is the dependence on the London penetration depth, λ.

CHAPTER 3. MAGNETIC VECTOR POTENTIAL METHOD

The use of the magnetic vector potential, **A** is a powerful tool for solving Maxwell's equations which has proven to be a mainstay approach for device level formulation including antenna, microwave, and optoelectronics as opposed to the traditional approaches we reviewed in the previous chapter. As described by Balanis [Balanis (1989)], there are two ways to specify an electromagnetic boundary-value problem. One way is the method we have just looked at, the current density method, which is a direct integration from **J** to **E** and **H**. The other method is the one that we will look at in this section, which is to determine **A** from **J** and then **E** and **H** from **A**. While the latter method may seem more involved, we will show that this form is actually mathematically simpler because of our freedom of gauge. This will be demonstrated using the same superconducting transmission line structure we have looked at previously. We believe that utilization of the magnetic vector potential to solve Josephson Junction problems will enable analytical closed form solutions to more complicated superconducting geometries that otherwise would require numerical techniques to solve. However, but not to contradict ourselves, we will look at numerical solution techniques as well for their versatility in obtaining realistic graphical solutions for complex and irregular geometries.

3.1 Introduction

The magnetic vector potential stems from the absence of free magnetic poles. This is most commonly exemplified by the following Maxwell equation:

$$\nabla \cdot \mathbf{B} = 0 \tag{72}$$

Due to this, **B** can then be written as the curl of another vector quantity since the divergence of a curl is zero.

$$\nabla \cdot \nabla \times \mathbf{A} = 0 \tag{73}$$

This vector is defined as the magnetic vector potential. We can easily determine both magnetic and electric fields quite simply from this quantity using equation (74).

$$\mathbf{B} = \nabla \times \mathbf{A}$$
$$\mathbf{E} = -\frac{\partial \mathbf{A}}{\partial t}. \tag{74}$$

The reason we introduce **A** is because both the electric and magnetic fields remain unchanged under a scalar transformation of **A**. This enables us to choose the form of **A** that is most convenient to work with in a given gauge. It is interesting to note here that from (74) **B** is not actually a true vector, but a psuedovector, since it is even under spatial inversion.

3.1.1 Calculation of the Magnetic Vector Potential

We now turn our attention to the calculation of the magnetic vector potential for a superconducting transmission line as discussed by Anderson, Mina, and Babaei Brojeny [Anderson et al. (2006)]. Again, we use the same geometry shown in Figure 1 and look at the TM^z case. Based on the symmetry of the problem we can choose a magnetic vector potential **A** such that A_z is the only nonzero component of the vector potential given by

$$A_z = X(x)Y(y)Z(z)\hat{z}. \tag{75}$$

We then solve the following wave equation to obtain the general form of the magnetic field potential in the three regions.

$$\nabla^2 \mathbf{A} + \omega^2 \mu\varepsilon \mathbf{A} = 0 \tag{76}$$

This equation holds provided that the divergence of **A** is zero. We use separation of variables to determine the general form of A_z. Earlier we had defined the current density traveling in the y-direction to be zero leading to $B_x = E_y = 0$. Using this and the relation between **B** and **A** given by (74) we have

$$B_x = \frac{\partial A_z}{\partial y} - \frac{\partial A_y}{\partial z} = 0. \tag{77}$$

Since we have already defined $A_y = 0$, we clearly see that

$$\frac{\partial A_z}{\partial y} = 0. \tag{78}$$

We can then use separation of variables with $A_z = X(x)Z(z)$. If we choose

$$\frac{1}{Z}\frac{\partial^2 Z}{\partial z^2} = -\kappa^2, \frac{1}{X}\frac{\partial^2 X}{\partial x^2} = -K^2, \text{ where}$$
$$\kappa^2 > K^2, \text{ and } K^2 + \omega^2 \mu\varepsilon = \kappa^2 \tag{79}$$

we have the following general solutions

$$Z(z) = e^{\pm i\kappa z}, \ X(x) = e^{\pm Kx}. \tag{80}$$

Selecting a $+z$ traveling solution and adding in the time dependence $e^{-i\omega t}$ we find the following solution for A_z

$$A_z = \left(ae^{k_x x} + be^{-k_x x} \right) e^{i(k_z z - \omega t)}. \tag{81}$$

This is obviously the vector potential given in the region of the insulating barrier, where $k_z^2 > k_x^2$ and leads to the dispersion relation

$$k_x^2 = k_z^2 - \omega^2 \mu\varepsilon. \tag{82}$$

Looking at the value of $k_z{}^2$ as a function of k_x at fixed ω we find the following

behavior shown in Figure 3 for a frequency of 100 x 10^9 rad/s.

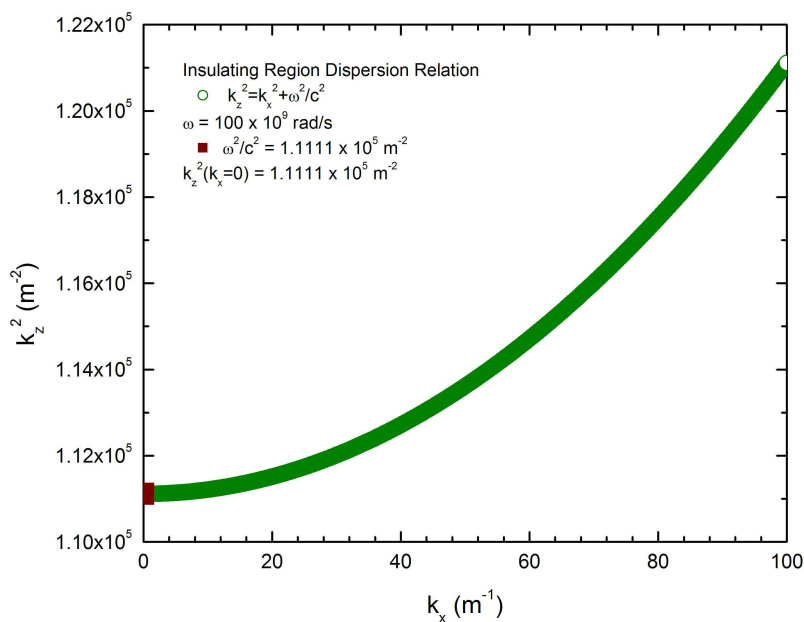Figure 3. Dispersion relation in the insulating region with $\omega = 100$ G-rad/s.

We see from the figure that at $k_x = 0$ the value of $k_z = \omega/c$ or in CGS units where $c = 1$, the

wavenumber is equal to the frequency. This is a familiar result and is expected. To take a

deeper look at the behavior of the dispersion relation we now look at the behavior as both k_x

and ω are varied.
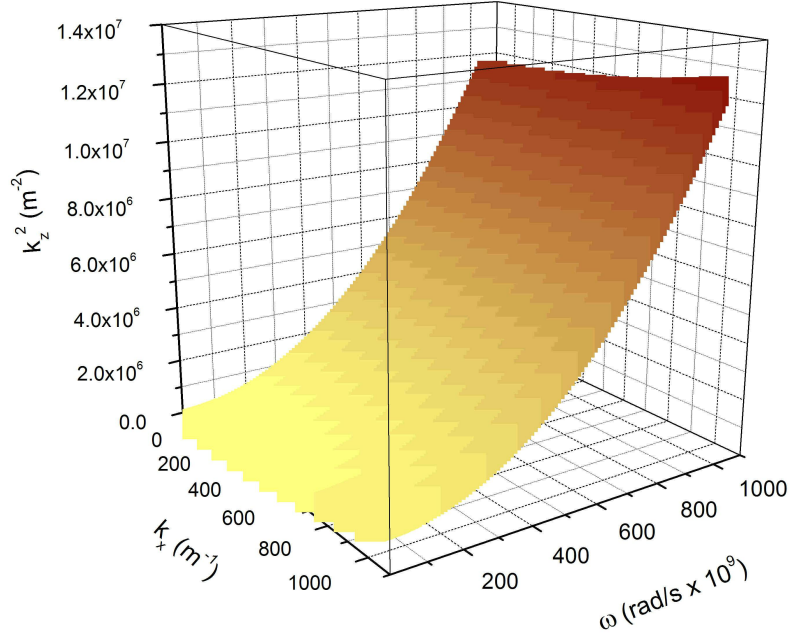
Figure 4. Dispersion relation for the insulating region with varying values of k_x and ω.

We see from the figure that this particular figure is one-quarter of a bowl type shape. The relative values of k_x to ω will distinguish the overall character of this figure. Here we have plotted using a ratio of k_x/ω ranging from 0 to 1×10^9 s/m. We have plotted in this way in order to see the $k_z(k_x = 0) = \omega/c$ value at a relatively realistic value of the angular frequency.

To keep our vector potential from diverging, the general form of the magnetic vector potential for the top and bottom superconductors is then given by

$$A_{z,top} = \left(be^{-k_x x} \right) e^{j(k_z z - \omega t)}$$
$$A_{z,bottom} = \left(ae^{+k_x x} \right) e^{j(k_z z - \omega t)} . \tag{83}$$

However, the divergence of **A** must vanish for both regions if we want to work in the Coloumb gauge, but this is not the case for the general solutions we derived. We must now apply a gauge transformation such that

$$\mathbf{A} \rightarrow \mathbf{A}' = \mathbf{A} + \vec{\nabla}\Lambda. \tag{84}$$

Where Λ is a scalar function chosen to make the divergence of **A** vanish and, after some trial and error, is found to be

$$\Lambda = \frac{ik_z}{k_x^2 - k_z^2}\left(ae^{k_x x} + be^{-k_x x}\right)e^{i(k_z z - \omega t)}. \tag{85}$$

Now, **A** for the insulating layer becomes

$$\mathbf{A} = \frac{ik_z k_x}{\omega^2 \mu\varepsilon}\left(ae^{k_x x} - be^{-k_x x}\right)e^{i(k_z z - \omega t)}\hat{x} + \left(1 - \frac{k_z^2}{\omega^2 \mu\varepsilon}\right)\left(ae^{k_x x} + be^{-k_x x}\right)e^{i(k_z z - \omega t)}\hat{z}. \tag{86}$$

Where $a = 0$ for the top superconductor and $b = 0$ for the bottom superconductor as we saw before. We can substitute this relation for **A** into (74) to determine the electric and magnetic fields in the dielectric region. Taking the curl of **A** we find

$$\mathbf{B} = -k_x\left(ae^{k_x x} - be^{-k_x x}\right)e^{i(k_z z - \omega t)}\hat{y}. \tag{87}$$

Taking the negative of derivative of **A** with respect to time we see that

$$\mathbf{E} = \frac{k_z k_x}{\omega\mu\varepsilon}\left(ae^{k_x x} - be^{-k_x x}\right)e^{i(k_z z - \omega t)}\hat{x} + \frac{ik_x^2}{\omega\mu\varepsilon}\left(ae^{k_x x} + be^{-k_x x}\right)e^{i(k_z z - \omega t)}\hat{z}. \tag{88}$$

Equations (87) and (88) are the electromagnetic equations for the insulating region of the superconducting transmission line. In order to get a detailed look at the behavior of the electromagnetic fields, we will look at their spatial and time dependence at a given frequency and wavenumber using the dispersion relation derived earlier. Using this dispersion relation we see that at a frequency of 100 G-rad/s and $k_x = 100$ m^{-1}, $k_z = 348$ m^{-1}. In order to simplify

the electromagnetic equations further, we will assume the values of *a* and *b* to be 1 in the insulating region. It is apparent from the electric field we derived that there are both real and imaginary components of the field. However, to get a representation of the wave, we will only concern ourselves with the real-space result. To do this, we will only observe the magnitude of the electric field $\sqrt{\mathbf{E} \cdot \mathbf{E}^*}$. Since the magnetic field is a real vector we will plot this field with no modification. We then find the following behavior shown below for the magnetic and electric fields in the insulating regime.
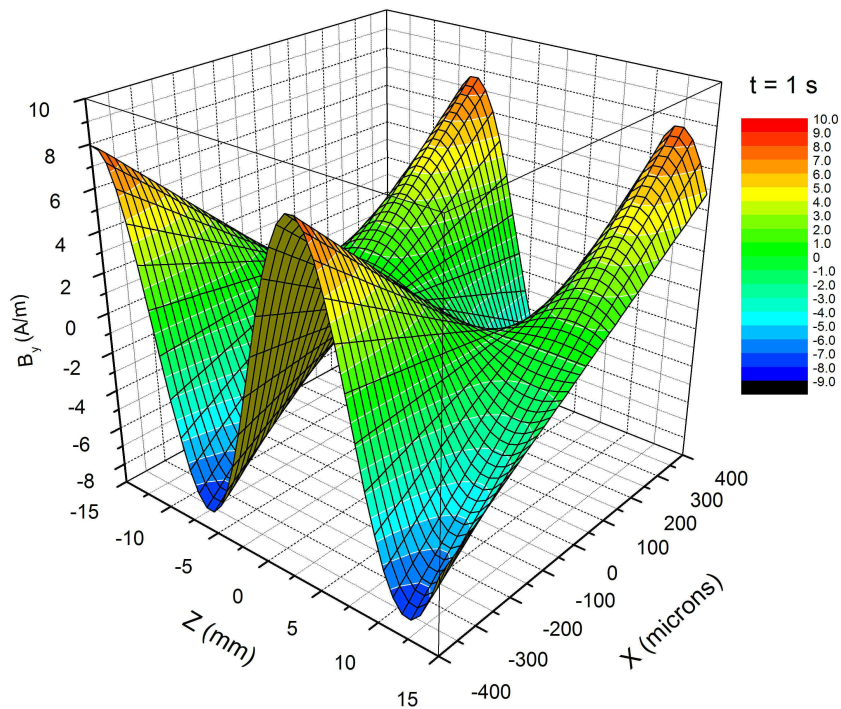
Figure 5. Magnetic field in the insulating region at t = 1s.
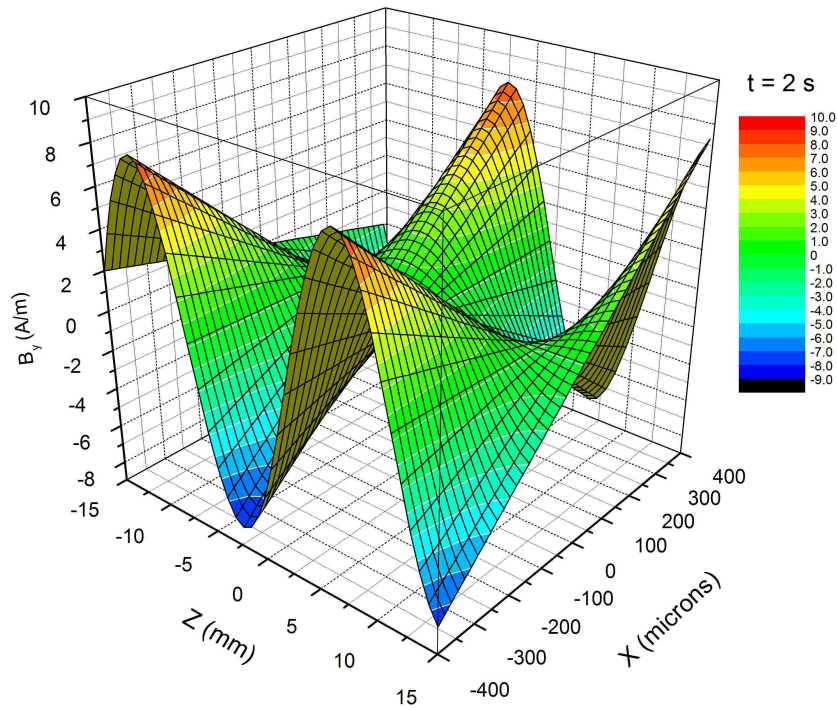
Figure 6. Magnetic field in the insulating region at t = 2s.
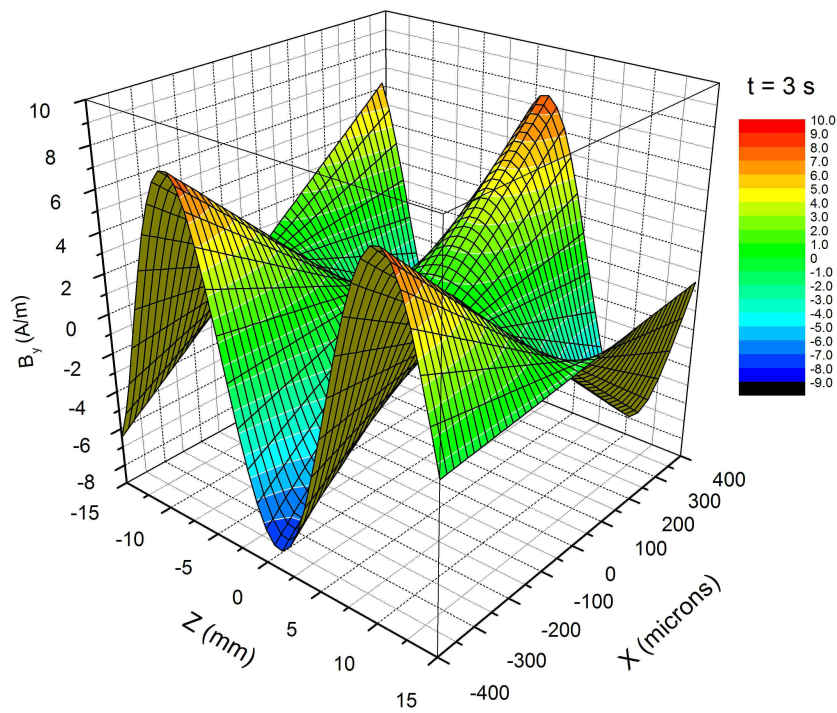
Figure 7. Magnetic field in the insulating region at t = 3s.
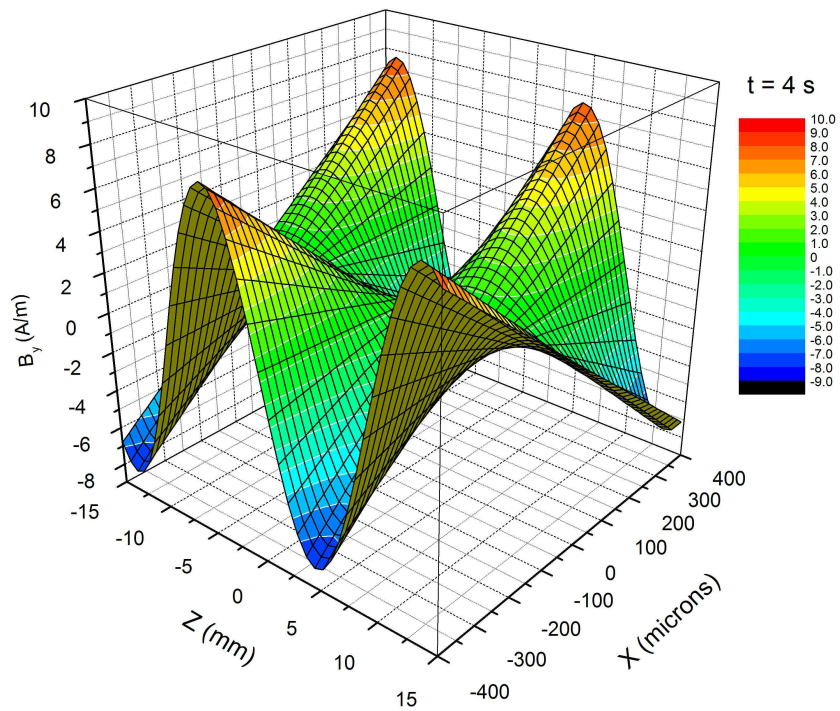
Figure 8. Magnetic field in the insulating region at t = 4s.
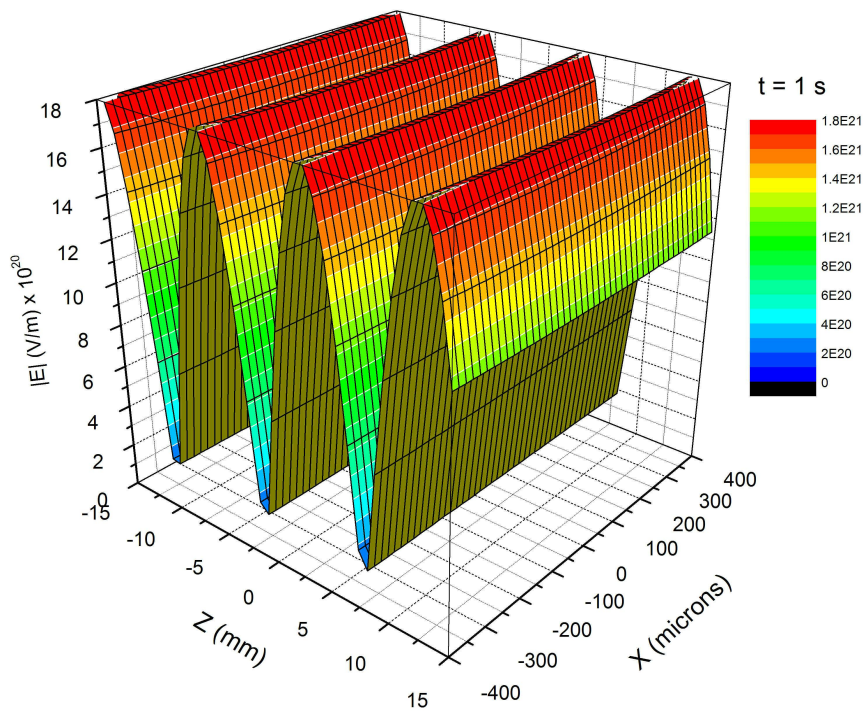
Figure 9. Electric field in the insulating region at t = 1s.
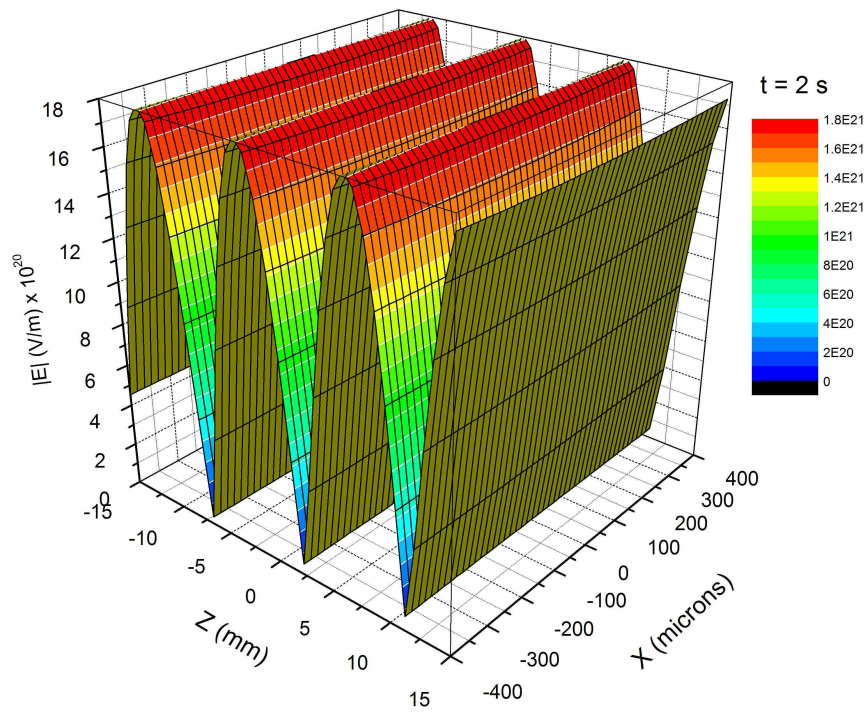
Figure 10. Electric field in the insulating region at t = 2s.
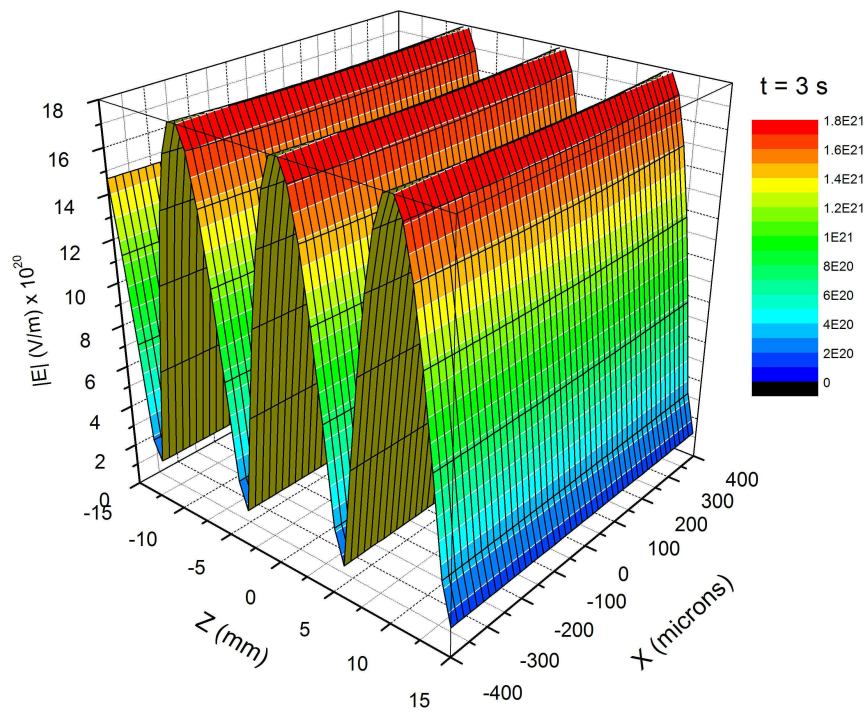
Figure 11. Electric field in the insulating region at t = 3s.
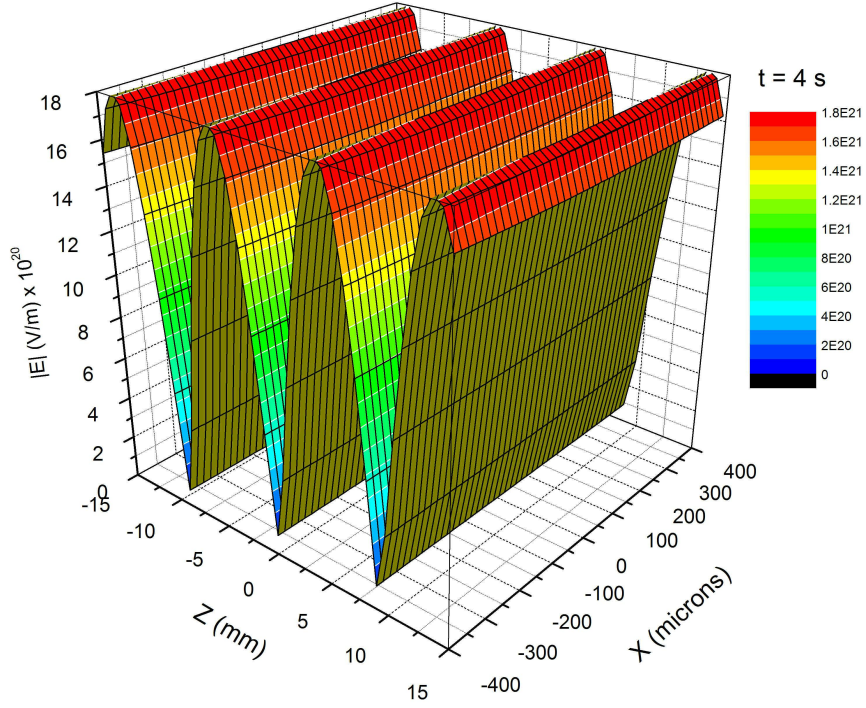
Figure 12. Electric field in the insulating region at t = 4s.

For the superconducting region of the transmission line structure, we use the

Helmholtz equation with a non-zero current since we have propagating currents in this

region. Equation (76) is rewritten as,

$$\nabla^2 A_z + \omega^2 \mu\varepsilon A_z = -\mu J, \tag{89}$$

where J is the current density in the superconducting region. The London equation relates

the current density to the magnetic vector potential for a superconductor.

$$J = -\frac{1}{\mu\lambda^2}\mathbf{A} \tag{90}$$

Here, λ is the London penetration depth given by

$$\lambda = \sqrt{\frac{\varepsilon m c^2}{n q^2}}. \tag{91}$$

In this equation, m is the mass, n the concentration, and q the charge. The London penetration depth is the thickness of the surface layer in which currents and magnetic fields can exist. General values for the London penetration depth are calculated to be about 4×10^{-6} cm for many elemental metals at absolute zero.

If we may digress slightly from our field calculations, it is interesting to note at this point that the magnetic field in the superconducting region should decay exponentially as [Ashcroft and Mermin (1976)]

$$B(x) = B_0 e^{-x/\lambda}. \tag{92}$$

We will see that this relation is indeed found in our solutions using the magnetic vector potential.

Resuming our prior calculation we find that by inserting (90) into (89) the following dispersion relation exists in the superconducting region.

$$k_x^2 = k_z^2 - \omega^2 \mu \varepsilon + \frac{1}{\lambda^2} \tag{93}$$

The dispersion relation found in (93) matches the dispersion relation found using current density method but using much simpler mathematics to do so. This relation is very similar to the dispersion relation found for the insulating region with the exception of the London penetration depth term. Still, this relation is simple enough that we can visualize the general form of it based on the result for the insulating region. Since we are working with a TM^z mode of propagation, our Helmholtz equation in the Lorentz gauge reduces to

$$\nabla^2 A_z + (\omega^2 \mu \varepsilon - \frac{1}{\lambda}) A_z = 0. \tag{94}$$

This is very similar to the Helmholtz equation we found in the insulating region with an extra term in the coefficient of A_z. Solving in a similar manner as previously, we determine that **A** at the top and bottom superconductors is given by

$$\mathbf{A}_{top} = \frac{-ik_z k_x}{\omega^2 \mu \varepsilon} d e^{-k_x x} e^{i(k_z z - \omega t)} \hat{x} + \left(1 - \frac{k_z^2}{\omega^2 \mu \varepsilon} - \frac{1}{\lambda^2 \omega^2 \mu \varepsilon} \right) d e^{-k_x x} e^{i(k_z z - \omega t)} \hat{z}$$

$$\mathbf{A}_{bottom} = \frac{ik_z k_x}{\omega^2 \mu \varepsilon} c e^{k_x x} e^{i(k_z z - \omega t)} \hat{x} + \left(1 - \frac{k_z^2}{\omega^2 \mu \varepsilon} - \frac{1}{\lambda^2 \omega^2 \mu \varepsilon} \right) c e^{k_x x} e^{i(k_z z - \omega t)} \hat{z}. \quad (95)$$

By factoring and rearranging terms we can write these equations more compactly as

$$\mathbf{A}_{top} = \frac{-ik_z k_x}{\omega^2 \mu \varepsilon} d e^{-k_x x} e^{i(k_z z - \omega t)} \left(\hat{x} + \left[1 - \frac{k_z^2}{\omega^2 \mu \varepsilon - \frac{1}{\lambda^2}} \right] \hat{z} \right)$$

$$\mathbf{A}_{bottom} = \frac{ik_z k_x}{\omega^2 \mu \varepsilon} c e^{k_x x} e^{i(k_z z - \omega t)} \left(\hat{x} + \left[1 - \frac{k_z^2}{\omega^2 \mu \varepsilon - \frac{1}{\lambda^2}} \right] \hat{z} \right). \quad (96)$$

In the above equations, the coefficients c and d can be written in terms of coefficients a and b using boundary conditions. To be thorough we confirm that the divergence of both the top and bottom superconductor magnetic vector potentials goes to zero.

$$\nabla \cdot \mathbf{A}_{top} = \frac{\partial}{\partial x} \left[\frac{-ik_z k_x}{\omega^2 \mu \varepsilon} b e^{-k_x x} e^{i(k_z z - \omega t)} \right] + \frac{\partial}{\partial z} \left[\left(1 - \frac{k_z^2}{\omega^2 \mu \varepsilon} - \frac{1}{\lambda^2 \omega^2 \mu \varepsilon} \right) b e^{-k_x x} e^{i(k_z z - \omega t)} \right]$$

$$= \frac{ik_z k_x^2}{\omega^2 \mu \varepsilon} b e^{-k_x x} e^{i(k_z z - \omega t)} + ik_z \left(1 - \frac{k_z^2}{\omega^2 \mu \varepsilon} - \frac{1}{\lambda^2 \omega^2 \mu \varepsilon} \right) b e^{-k_x x} e^{i(k_z z - \omega t)} \quad (97)$$

$$= \frac{ik_z}{\omega^2 \mu \varepsilon} b e^{-k_x x} e^{i(k_z z - \omega t)} \left(k_x^2 - k_z^2 + \omega^2 \mu \varepsilon - \frac{1}{\lambda^2} \right)$$

Using (93) it is clear that the quantity on the final line in parenthesis is equal to zero, confirming that the divergence of **A** does indeed go to zero. By a similar solution, the divergence of $\mathbf{A}_{bottom}$ goes to zero.

Using the relations found in (74), the magnetic and electric fields can be determined in the same way as in the insulating layer. After taking the curl of the magnetic vector potential and rearranging terms, we find the following relation for the magnetic field for the top and bottom superconductors.

$$\mathbf{B}_{top} = \frac{k_z k_x}{\omega^2 \mu \varepsilon} d e^{-k_x x} e^{i(k_z z - \omega t)} \left[k_z - i k_x + \frac{i k_z^2 k_x}{\omega^2 \mu \varepsilon - \frac{1}{\lambda^2}} \right] \hat{y}$$

$$\mathbf{B}_{bottom} = \frac{k_z k_x}{\omega^2 \mu \varepsilon} c e^{k_x x} e^{i(k_z z - \omega t)} \left[\frac{i k_z^2 k_x}{\omega^2 \mu \varepsilon - \frac{1}{\lambda^2}} - i k_x - k_z \right] \hat{y}$$

(98)

We can also use the dispersion relation (93) to rewrite these equations in varying forms. From equation (98) we see that since k_x is a function of $1/\lambda$, the magnetic field inherently decays as a function of the London penetration depth as discussed earlier.

In order to obtain a physical representation of the spatial and time dependence of the magnetic field, we look at the spatial dependence of the magnetic field at selected times. By symmetry, the top and bottom magnetic field equations should yield the same result, so we will focus on the magnetic field for the top of the structure. To get a realistic sense of time dependence we use a frequency of 100 G-rad/s, which is in the range of a typical Josephson frequency. This frequency value gives rise to a Josephson length of 150 μm, which is equivalent to the London penetration depth, but for a Josephson junction. For consistency we will use the same values of wavenumbers that we used in the insulating layer and set all other general constants equal to 1. In order to look at the real component of the magnetic field we

consider the magnitude in the same manner as we did for the electric field before. The

following shows the results of these simulations.

Figure 13. Magnetic field in the superconducting region at t = 1s.

Figure 14. Magnetic field in the superconducting region at t = 2s.

Figure 15. Magnetic field in the superconducting region at t = 3s.

Figure 16. Magnetic field in the superconducting region at t = 4s.

Now, we derive the Electric Field equations using the magnetic vector potential and equation (74). Taking the negative of the derivative of **A** with respect to time we find the following equations for the top and bottom superconductor electric fields.

$$\mathbf{E}_{top} = \frac{k_z k_x}{\omega\mu\varepsilon} d e^{-k_x x} e^{i(k_z z - \omega t)} \left(\hat{x} + \left[1 - \frac{k_z^2}{\omega^2 \mu\varepsilon - \frac{1}{\lambda^2}} \right] \hat{z} \right)$$

$$\mathbf{E}_{bottom} = \frac{-k_z k_x}{\omega\mu\varepsilon} c e^{k_x x} e^{i(k_z z - \omega t)} \left(\hat{x} + \left[1 - \frac{k_z^2}{\omega^2 \mu\varepsilon - \frac{1}{\lambda^2}} \right] \hat{z} \right)$$

(99)

In a similar manner we can obtain a visualization of the spatial and time dependence of the electric field equations using the same simplifications and values used to plot the magnetic field previously.
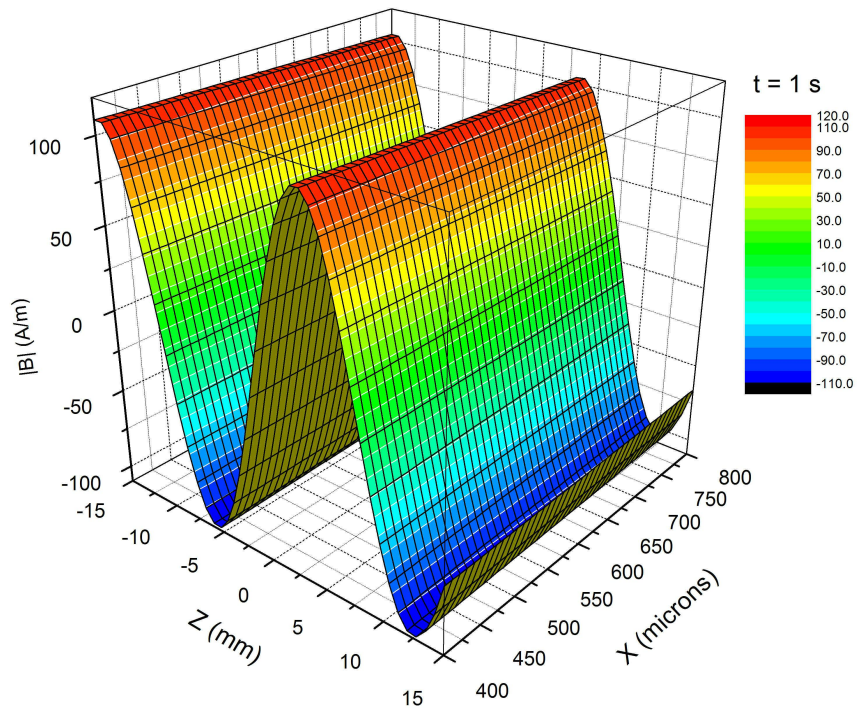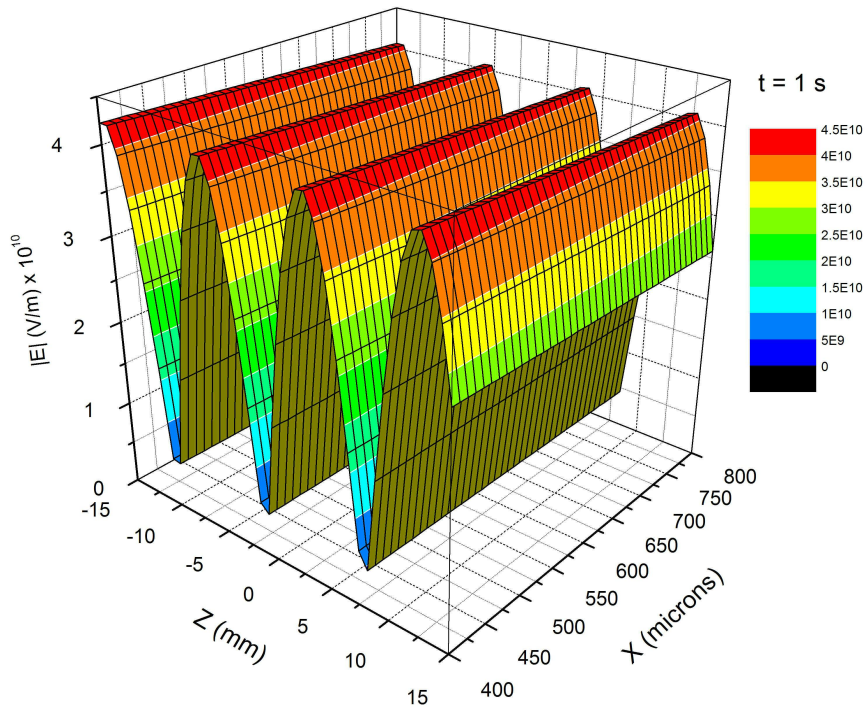
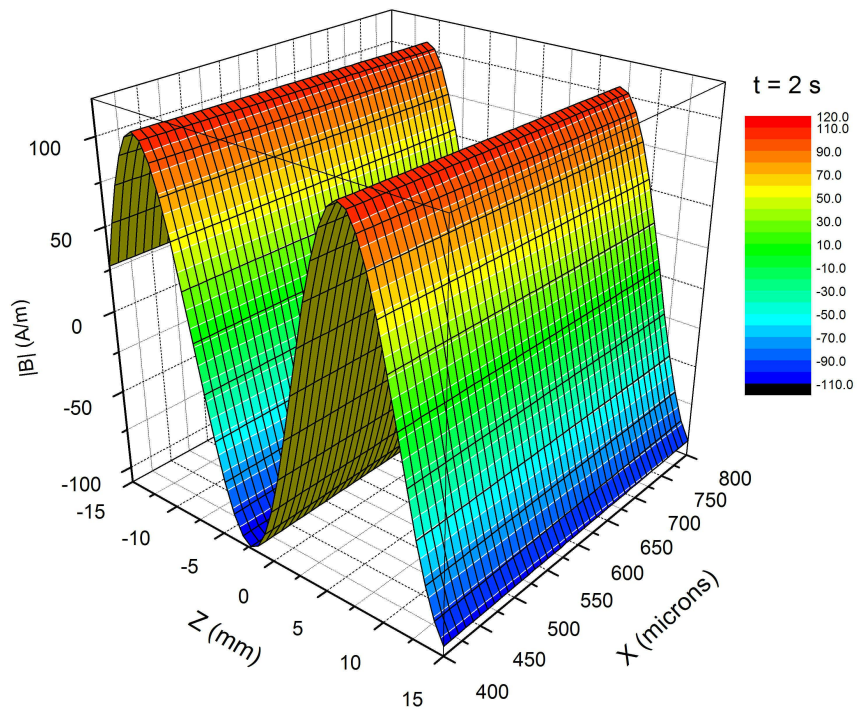Figure 17. Electric field in the superconducting region at t = 1s.
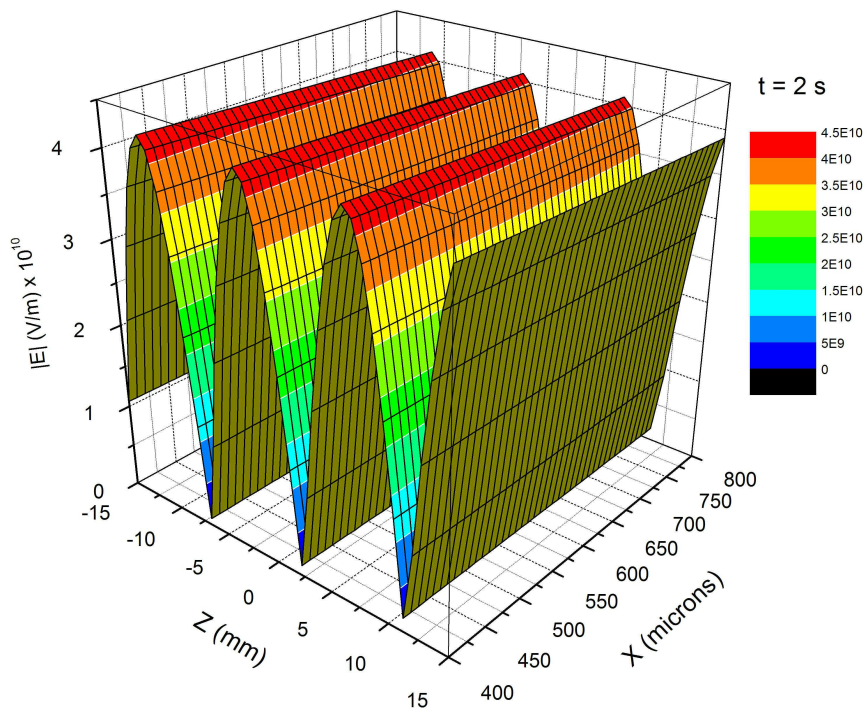
Figure 18. Electric field in the superconducting region at t = 2s.

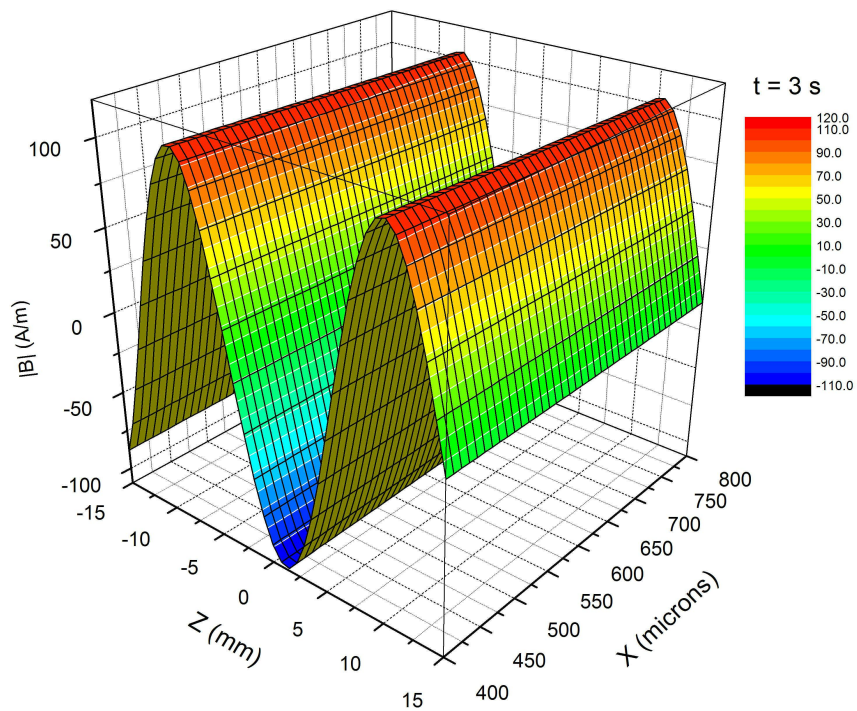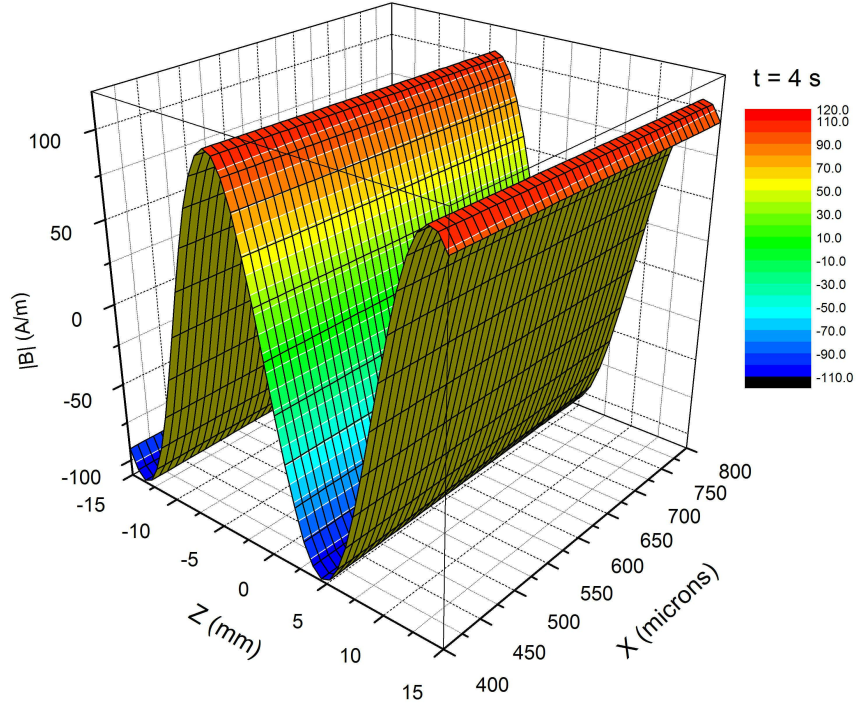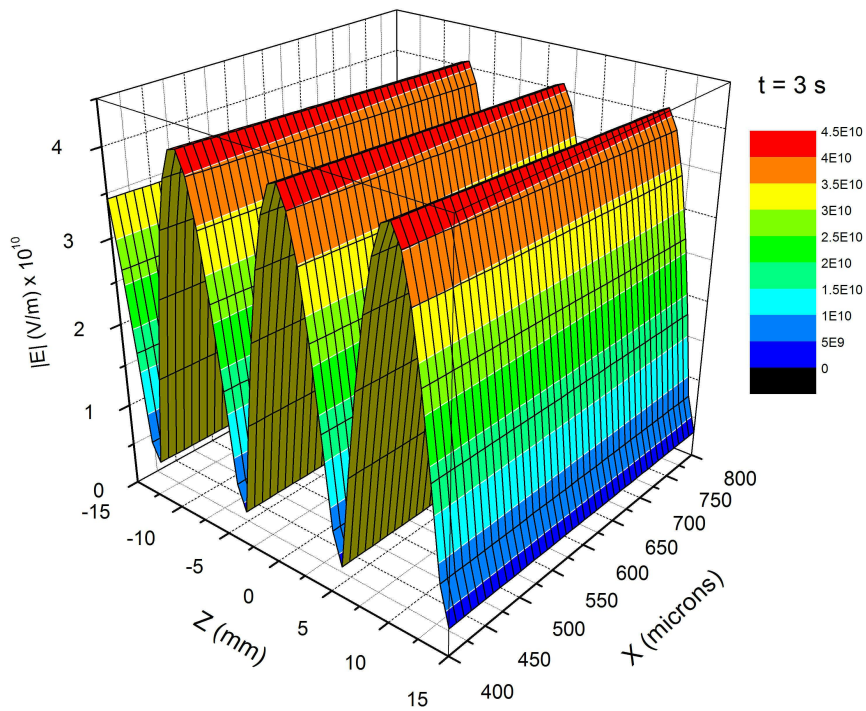Figure 19. Electric field in the superconducting region at t = 3s.
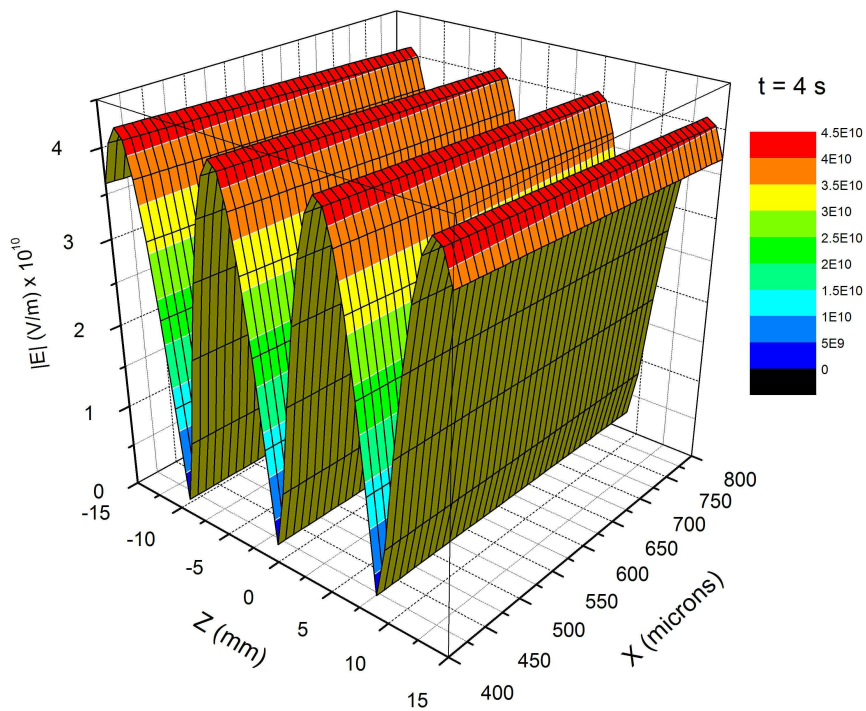
Figure 20. Electric field in the superconducting region at t = 4s.

3.1.2 Summary of Solution

In this section we have calculated the dispersion relation, magnetic vector potential, and electromagnetic field equations for the insulating and superconducting regions of the superconducting transmission line depicted in Figure 2. We have shown that by using the magnetic vector potential we can derive the same result for the dispersion relation for these regions as derived by the methods reviewed in chapter 2. We also found closed form solutions for the propagating fields of the superconducting transmission line structure. These fields were then simulated using a Matlab script in order to obtain a realistic view of the behavior of these fields. We will continue to build upon these results by considering the coupling between the superconductors in the following sections.

3.2 The Josephson Current

In the previous section we looked at the solution of the electromagnetic fields for superconductors separated by an insulating boundary without taking into account any quantum effects. As we discussed earlier, the Josephson current is represented by $J = J_c \sin(\phi)$, where J_c is the superconducting critical current and ϕ is the phase difference across the boundary. In the situation we are considering, we have a constant DC bias being applied across the junction via an external magnetic field. The superconducting current is then simply given by the AC Josephson effect

$$J = J_0 \sin\left[\delta(0) - \left(\frac{2eVt}{\hbar}\right)\right] \tag{100}$$

The problem we are now faced with is one of solving equation (89) with the above current substituted. In the following section we will look at the Sine-Gordon equation which

describes the coupling between superconductors, and attempt to solve for the electromagnetic fields across the boundary using the finite difference method. We will also go beyond our original objectives and discuss how using the finite difference method may be a more modular solution method for probing Josephson junction structures having unique geometries, defects, and inhomogeneities.

3.2.1 Sine-Gordon Equation

The non-stationary Sine-Gordon equation is given by

$$\nabla^2 \phi - \frac{1}{v^2} \frac{\partial^2 \phi}{\partial t^2} = \frac{1}{\lambda_J^2} \sin \phi. \qquad (101)$$

Where v is the junction velocity and λ_J is the Josephson length. This equation describes the phase difference or coupling across the boundary between superconductors. We will now compare the numerical solutions between both the non-stationary version of the Sine-Gordon and the stationary or linear version in order to obtain a realization of the coupling occurring across the insulating barrier. This comparison will enable us to determine the time scale at which the linear approximation remains valid. The linear Sine-Gordon equation is simply determined using the small angle approximation where $\sin \varphi \rightarrow \varphi$ and is given by

$$\nabla^2 \phi - \frac{1}{v^2} \frac{\partial^2 \phi}{\partial t^2} = \frac{1}{\lambda_J^2} \phi. \qquad (102)$$

Since the Sine-Gordon equation ignores dissipative effects, we only need to determine the value of the velocity v and the Josephson penetration depth λ_J. The Josephson length should not be confused with the London penetration depth, λ. The Josephson length is

due to screening caused by supercurrents in the junction and is about 4 orders of magnitude

larger than the London penetration depth. These two quantities are then expressed as

$$v = c \left(\frac{1}{4\pi CD} \right) \tag{103}$$

Here C is the capacitance per unit area of the junction and D is the layer thickness.

The value of v is generally of the order $c/20$. The Josephson length is defined as,

$$\lambda_J = \frac{v}{\omega_J} \tag{104}$$

The value of the Josephson frequency, ω_J, is generally of the order of 100 GHz giving us a

value of 150 μm for the Josephson length. Using these values and ranging over a value of

300 μm in the z direction and looking over a period of 0.01 s we see the following result

using ϕ with a general form of $\phi = e^{j(kr-\omega t)}$ where $k = 1$ for this simulation. Figure 21A is

the result using the non-equilibrium equation and figure 21B is the result assuming small

oscillations.
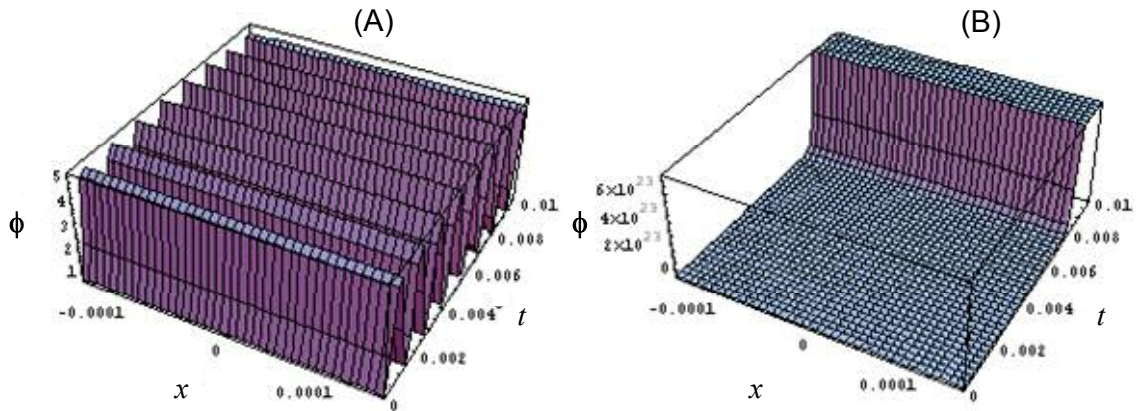
Figure 21. Plot of the solution to the non-stationary (A) and stationary (B) Sine-Gordon

equations for $0 < t < 0.01$s.

In Figure 21 we see an incredibly large discrepancy between the non-linear 21A and linear 21B results. This does not mean, however, that our small oscillation model is incorrect. If we narrow our time scale down by a factor of 100 we see the following results for the non-linear solution 22A and the linear solution 22B.
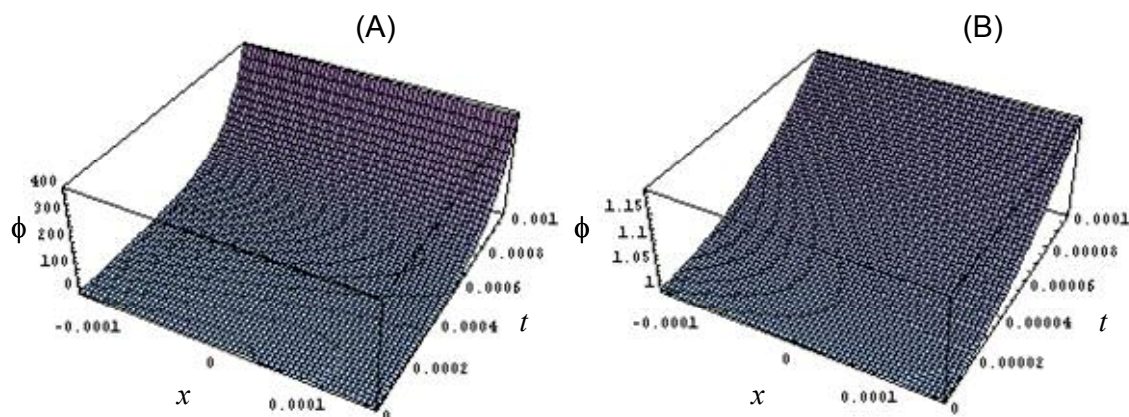
Figure 22. Plot of the solution to the non-stationary (A) and stationary (B) Sine-Gordon equations for $0 < t < 0.0001$s.

If we look at the maximum amplitudes in Figure 22 we see about a 4.2% difference in the $\phi(t = 0.0001$ s$)$ results. This gives us an indication of the time scale over which the linear model remains valid for this frequency and what is meant by small oscillations. From this exercise we can determine that the linear equation will yield a less than 5% difference for radiation with frequencies greater than 10 kHz. What is interesting to note is the fact that the time scale seems to be the main determining factor in whether or not the linear equation is a good approximation. This means that coupling across the barrier is better described by the linearized Sine-Gordon equation for higher frequencies, and is the reason why this model is in such good agreement with experimental results for these applications.

It might seem that the length of the barrier has no effect on the validity of the linearized equation, but this is far from the truth. The length of the barrier plays a vital role in the behavior of our transmission line. Its main constraint, however, is that the length of the barrier must be smaller than the dephasing length in order for coupling between the superconductors to even occur. It is this constraint that makes D small enough that the linear equation is a good approximation only for high-frequency applications. This implies that if the penetration depth were sufficiently large, the linear equation would also be reasonable to use for lower frequency modeling as well. This is important since the linear equation has been used in the development of much of today's useful technology employing Josephson junctions. It is important to realize that even though this equation models the behavior of many of these applications quite well, it is still an approximation and may have limitations in modeling future technologies.

3.2.2 Solution Using the Josephson Current

As we stated earlier, we now look at the solution of equation (89) using the current derived for the AC Josephson effect. Inserting the current from equation (17) we find

$$\nabla^2 A_z - \frac{\partial^2 A_z}{\partial t^2} = -\mu J_0 \sin\left[\delta(0) - \left(\frac{2eVt}{\hbar}\right)\right] \tag{105}$$

If we assume $\delta(0) = 0$, then the basic form of the differential equation we are trying to solve with the Josephson Current is

$$\frac{\partial^2 A}{\partial z^2} - \frac{\partial^2 A}{\partial t^2} = -\mu J \sin(\omega t) \tag{106}$$

where, $\omega = 2eV/\hbar$. Solving this system in the same manner we did before now becomes much more difficult because of the transcendental equation. Instead, we turn to numerical techniques to simplify the problem.

The form of the second order derivatives from the forward difference formula are given by

$$\frac{\partial^2 A}{\partial z^2} = \frac{A(i+2, j) - 2A(i+1, j) + A(i, j)}{(\Delta z)^2} \text{ and,} \tag{107}$$

$$\frac{\partial^2 A}{\partial t^2} = \frac{A(i, j+2) - 2A(i, j+1) + A(i, j)}{(\Delta t)^2}. \tag{108}$$

The backward difference formula yields the following second order derivatives

$$\frac{\partial^2 A}{\partial z^2} = \frac{-A(i-2, j) + 2A(i-1, j) - A(i, j)}{(\Delta z)^2} \text{ and,} \tag{109}$$

$$\frac{\partial^2 A}{\partial t^2} = \frac{-A(i, j-2) + 2A(i, j-1) - A(i, j)}{(\Delta t)^2}. \tag{110}$$

Using the central difference formula, the form of the second order derivatives in the equation above can be re-written as

$$\frac{\partial^2 A}{\partial z^2} = \frac{A(i+1, j) - 2A(i, j) + A(i-1, j)}{(\Delta z)^2} \text{ and,} \tag{111}$$

$$\frac{\partial^2 A}{\partial t^2} = \frac{A(i, j+1) - 2A(i, j) + A(i, j-1)}{(\Delta t)^2}. \tag{112}$$

Substituting the central difference forms of the second derivatives into equation (106) we find

$$2A(i, j)\left(\frac{1}{(\Delta z)^2} - \frac{1}{(\Delta t)^2}\right) = -\frac{A(i+1, j) + A(i-1, j)}{(\Delta z)^2} + \frac{A(i, j+1) + A(i, j-1)}{(\Delta t)^2} \tag{113}$$
$$- \mu J \sin(\omega j).$$

If we let $\Delta z = \Delta t$, this equation can be reduced even further having the form

$$A(i+1,j)+A(i-1,j)-A(i,j+1)-A(i,j-1) = -(\Delta z)^2 \mu J \sin(\omega j). \qquad (114)$$

This is then the equation that governs the form of A in the insulating region between the two superconductors when the barrier thickness is such that the AC Josephson effect is present. In the superconducting region we simply replace the equation for the current density with the relation found in equation (90) and equation (114) becomes

$$A(i+1,j)+A(i-1,j)-A(i,j+1)-A(i,j-1) = (\Delta z)^2 \frac{1}{\lambda^2} A(i,j). \qquad (115)$$

We can use the fact that J=0 in purely insulating regions where the spacing between superconductors is too great for coupling between the barrier to occur. In this way we can introduce defects and other types of random surface and boundary effects that would otherwise be too difficult to solve by hand. Using these equations for the magnetic vector potential we can apply the iterative finite difference method to calculate A. In this way, we can study different geometries and create defects in the junctions by purely changing the current density for that particular region.

To begin, we need to set up the structure of our Josephson junction. The preliminary Matlab script for this initialization is found in Appendix C. We begin our simulation by considering a single junction comprised of only 2 homogeneous and isotropic superconductors separated by a thin homogenous and isotropic insulating layer. We will take a 2-D slice in the middle of the structure to eliminate the need to take into account surface effects from above or below the plane under consideration. A major part of this initialization process is to incorporate the boundary conditions. Since we will again be looking in the xz-plane as a function of time, we will specify continuous boundary conditions in the z-direction

and purely insulating boundary conditions on the surface of our superconductors. Since we will be simulating the fields of this structure under the conditions of the AC Josephson effect, we will need to take into account the current due to the externally applied magnetic field. For the purposes of the simulation we will constrain this current to the surface of our superconducting region.

In order to determine this current we use the relation between magnetic field and current density in an infinite conductivity media given by Balanis [Balanis (1989)].

$$\hat{n} \times \left(H_2 - H_1 \right) = J_s \tag{116}$$

Here H_1 and H_2 are the values of the tangential magnetic field on either side of the surface, J_s is the surface current density, and $\hat{n}$ is a unit vector perpendicular to the surface. For our simulation we will let the difference between tangential components of the magnetic field across the boundary be 5 A/m, and thus the current density will be 5 A/m. This external magnetic field will be a constant DC field so we will constrain the surface current density to this value for the duration of the simulation.

Using this setup and initial conditions, we develop a solution using the iterative finite difference method. We define a square mesh of 200 x 200 points in the x-direction and in time as an initial setup. In the future we will expand into the z-direction as well to create a cubic mesh from which we can extract cross sections and develop movies as we did in our transmission line solution earlier. In our simulation, *dx* and *dt* represent the size of the space and time elements respectively. These quantities are set equal, as described above, to simplify our calculation. The successive-over-relaxation method is used to iteratively solve for the magnetic vector potential throughout the mesh as outlined by Sadiku [Sadiku 2001]. In order to use this method we define the following residual

$$R = A(i-1, j) + A(i+1, j) - A(i, j-1) - A(i, j+1) + \mu \cdot dx \cdot dt \cdot A(i, j) \qquad (117)$$

for the insulating region. For the superconducting region we then have

$$R = A(i-1, j) + A(i+1, j) - A(i, j-1) - A(i, j+1) - \mu \cdot dx \cdot dt \cdot J \cdot \cos(f \cdot j). \qquad (118)$$

The magnetic vector potential can be calculated at each mesh point using $R(i, j)$ for

the nth iteration multiplied by a convergence factor ω to increase the convergence rate as seen

in (119).

$$A^{n+1}(i, j) = A^n(i, j) + \frac{\omega}{4} R^n(i, j) \qquad (119)$$

Generally convergence factors between 1 and 2 are used. As convergence is reached

$R(i, j)$ tends to zero, and when the average value of $R(i, j)$ is below 1.0×10^{-5} for a given

iteration, convergence is considered reached.

The following figure shows the initial setup of the geometry of the junction we are

considering in space and time.
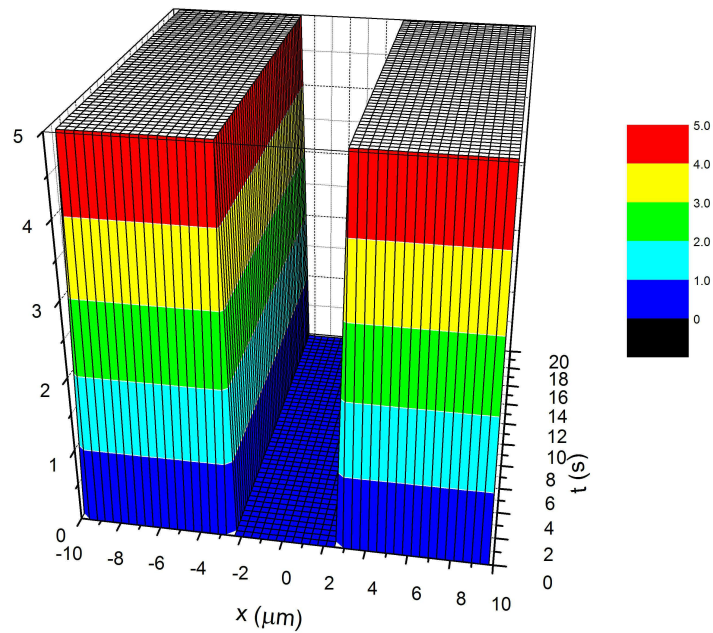
Figure 23. Space-time geometry of the Josephson junction under consideration.

From this figure we see both superconductors separated by an insulating layer in the x-direction, and this geometry is continuous in time. Finally, the electromagnetic fields can be determined from this method using numerical derivative techniques. In this way visual solutions can be obtained for the electromagnetic fields of the structure in space and time.

Using the finite difference method is a powerful tool for solving for the electromagnetic fields of Josephson junction structures and allows us the freedom to add many factors to our simulations. Here, we have laid the foundation for a solution method using the finite difference method. In the future there we foresee great challenges in the further development of this method for characterization and defect analysis.

CHAPTER 4. SUMMARY AND DISCUSSION

We began our efforts with the motivation for finding a novel solution method for a superconducting transmission line and Josephson like structures in order to better understand their behavior and to hopefully begin efforts that would eventually lead to a defect characterization technique in such structures. We formulated a solution method for a superconducting transmission line using the magnetic vector potential as a starting point. This solution method allowed us to find closed form solutions of the electromagnetic field equations and to view these solutions graphically using realistic values for the frequency and wavenumber as determined from the dispersion relation. The example we presented of a planar geometry transmission line consisting of two superconducting regions separated by a thin insulating region is a simple starting point showing the viability of this option as a solution method for similar structures of different geometries and initial conditions.

4.1 Summary of Work

In the preceding sections we began by reviewing the work of Josephson and the events leading up to his discovery of the Josephson junction. It was this work on the coupling between superconductors separated by a thin non-superconducting layer that has led to an increasingly large body of research on superconducting devices. More recently, it was the work by Wu and others that re-kindled the interest in the investigation of the electromagnetic fields of a superconducting layered device and was the starting point of the research in this paper. It was from this point that we began looking at the common methods used to solve for the electromagnetic fields of such a structure as discussed earlier in Section

2.2. After reviewing these methods, it was hypothesized that using the magnetic vector potential may be a simpler way to obtain the same result.

Using the magnetic vector potential as a starting point with a transverse magnetic to z mode of propagation, the electromagnetic fields for the superconducting and insulating regions of the superconducting transmission line were calculated. These results were explored further by looking at the physical representation of these fields in space and time. Next, we explored the Sine-Gordon equation in an attempt to better understand the coupling of a Josephson junction before diving into the problem of solving for the electromagnetic fields of a Josephson junction. Finally, we concluded our work by beginning to look at the solution for the electromagnetic fields in a Josephson junction by using the current for the AC Josephson effect that we had evaluated earlier. Our attempt at this solution utilized calculating the magnetic vector potential using the finite difference method. In this way we believed we could solve for very complex geometries that ordinarily could not be solved by hand. It is then our hopes to expand on this method in order to develop a modular function to solve for the fields Josephson-type structures.

4.2 Discussion of Results

We began our new work by looking at the insulating region of the superconducting layered structure depicted in Figure 2. Our initial result showed that we can obtain the same dispersion relation seen in equation (81) using the magnetic vector potential as we saw before in section 2 using other methods. Looking at this equation graphically, we saw in Figure 4 that the generic shape of $k_z{}^2$ as a function of k_x and ω was that of a bowl in three dimensions. This result is useful in our simulations of the electromagnetic fields where we can then use

realistic values of the wavenumbers and frequency in our results to obtain a physical representation of these fields. This result for the dispersion relation was what we expected based on previous results.

In addition to the dispersion relation, we carried out our formulation further in order to obtain the magnetic vector potential using the Coulomb gauge and from there the resultant electromagnetic fields using Maxwell's equations. In Figures 5 – 8 we looked at the y-component of the magnetic field as a function of space and time. We must note here that the data in the figures were simulated using a constant value of time and what we have plotted is the value of the magnetic field in the xz-plane. In these figures we see a wave propagating in the z-direction with a zero value in the middle of the insulating region. This is what we would expect. From the magnetic field equation we derived in (87), we clearly see a propagation term in the z-direction. Also, if we were to set x = 0, we would have a zero result provided constants *a* and *b* were equal. In the case of our simulation these were both set to 1 for simplicity, but would normally be determined by a set of initial conditions.

Our result for the electric field in this region was given by equation (88) and simulated in Figures 9 – 12 in the same manner as the magnetic field. Here we plotted the magnitude of the electric field so imaginary components could be neglected, and to consider a term relating to the energy of the electric field. The energy density of the electric field is given by

$$w_E = \frac{\varepsilon}{2} |\mathbf{E}|^2 . \qquad (120)$$

Again in Figures 9 – 12 we see a wave propagating in the z-direction, which is consistent with the equation we derived. We see from the figures that at a given z-position

the value of the electric field is constant across the insulating barrier. This is to be expected since this region is similar to the region in a parallel plate capacitor, where the electric field is also constant between the plates. In this case the plates are our superconductors.

Moving on to the superconducting region, we used the same method as for the insulating region, but using the current for the superconducting region. Our results for the electromagnetic fields for the top and bottom superconductors are then summarized by equations (98) and (99). We again look at the magnetic field first.

In this case, since we have imaginary components of the magnetic field, we simplify the result by simulating the magnitude of the magnetic field as we did for the electric field earlier. In the case of the magnetic field, the energy density is given by

$$w_B = \frac{1}{2\mu}\left|\mathbf{B}\right|^2 . \tag{121}$$

Figures 13 – 16 depict the magnetic fields in the top superconducting layer in the xz-plane for times of 1s, 2s, 3s, and 4s. The propagation of the magnetic field in the superconducting layer is consistent with that seen in the insulating layer as expected. What is not consistent between the two regions is the phase. We note that the minimum and maximum values do not align along the insulating/superconducting boundary as one would expect. We do note, however, that these fields were not plotted in the same manner. While we are looking at the magnitude of the magnetic field in the superconducting layer, we looked at the actual magnetic field in the insulating layer. Perhaps if we compared apples to apples in this case we would have a better comparison of this quantity. We will get a better idea of the possible cause of this phenomenon when we look at the comparison of the electric fields in the two

regions. Finally, we note that the magnitude of the magnetic field does indeed decrease as expected as we move in the x-direction.

Turning now to the electric fields in the superconducting region, we look at figures 17 – 20. We see, as we have for all of the fields so far, that the electric field is propagating in the z-direction. In this case, we do not see a phase difference between the insulating and superconducting regions. This leads us to believe that the difference in representation of the magnetic fields is the cause of the apparent shift in phase, however, more work is necessary to verify this but will not be carried out here since this is not the focus of our efforts. It may be possible that in calculating the magnitude of the magnetic field, we have somehow mixed in the phase due to the imaginary component we were trying to eliminate. Returning to our discussion of the electric field, we note that the electric field also shows a decaying behavior as it penetrates into the superconductor. Looking at our solution to the superconducting transmission line problem, we see that we have successfully calculated the electromagnetic fields of this structure using the magnetic vector potential as a mathematical tool to eliminate the need for direct integration.

Building upon our work on the superconducting layered transmission line, we consider a similar structure, but one in which the spacing between superconductors is sufficiently small enough for coupling across the barrier to occur as predicted by Josephson. In this case we used the Sine-Gordon equation to probe this coupling. By solving both the linear and non-linear forms of the Sine-Gordon equation we were able to gain insight into the time scale over which the linear approximation remains valid.

From our results it is apparent that the linear approximation is a good approximation on very short time scales, or in other words very high frequencies. This bodes well for the

work being done on Josephson devices. Since current efforts are focused on the fast switching of such devices the linear approximation is a logical way to simplify simulations of the coupling effects of such devices. This enables accurate results with much simpler computation.

Finally, our analysis of the superconducting layered structure introduced all the way back in Figure 2 led us to the problem of again solving for the electromagnetic fields of the structure, but this time taking into account the coupling between superconductors in the form of the AC Josephson current. To this end, we again use an approach involving the magnetic vector potential, but this time we formulate a numerical solution using the finite difference method. Our basic solution scheme is summarized in Section 3.2.2. A summary of the necessary future steps is given in the following chapter. Appendix C also contains sample Matlab scripts used to setup the problem. We have presented an initial step in forming a modular function to simulate the electromagnetic fields of a Josephson junction to develop a method of characterization. It is our hope that this characterization method could ultimately be used to study defects in Josephson junctions in order to perform in situ calibration of devices using Josephson junction technology.

CHAPTER 5. FUTURE DIRECTIONS

With the work that we have completed and the discussion above there are some obvious directions for our research to take. The most notable is the forward development of our numerical solution for the electromagnetic fields of a Josephson junction using the finite difference method. In this chapter we will discuss the necessary future steps to complete the solution. Next, we will look at the expansion of our solution for the electromagnetic description of a superconducting transmission line using the magnetic vector potential. As we discussed earlier we believe that this method could easily be adapted to different geometries with similar results. Here, we will discuss logical future steps in the expansion of this method. Lastly, we will consider the many quantities and simplifications we made along the way and discuss their possible impact and the way that they may be incorporated possibly leading to a more accurate solution to the problems we have discussed thus far in this paper.

5.1 Josephson Current

We presented a setup of the formulation using the finite difference method to solve for the electromagnetic fields of a Josephson junction. While the basic structure and equations of this method were laid out and defined, work is still necessary to further develop this technique. Boundary conditions need to be appropriately applied and the numerical derivatives defined in order to calculate the electromagnetic fields.

There are many paths that can be taken with our finite difference routine. One is to refine the script and take into account other factors such as varying the frequency and wavenumber, and even considering imaginary components of these quantities. The path that we are most interested in, however, is looking at defects in the Josephson structure. In order

to accomplish this, a more tedious task of possibly manually creating a mesh of different regions and current dependencies may be necessary. In this way we can explore defects in both the superconducting and insulating regions such as vortices, or regions where coupling across the boundary may not occur.

In addition, we can look at more exotic Josephson junction geometries. This would then be a simple way to create new geometries and test for novel properties before synthesizing an actual junction. As we noted in our initial case we are only considering a single junction. Future simulations would take into account many junctions, possibly of different sizes and boundaries. Ultimately we would build toward our goal of being able to characterize actual Josephson devices in order to study their electromagnetic properties in order to make more useful and precise devices.

5.2 Higher Complexity Geometries

In our solution method in Section 3.1, we solved for the magnetic vector potential in planar coordinates for a TM^z polarization, and later calculated the electromagnetic equations from this vector potential. While our results were interesting, there is a multitude of other situations we could explore using this same method. Staying within the same basic geometry, we can begin looking at different initial conditions by looking at different modes of propagation. While other transverse magnetic TM modes are just rotations of our coordinate system, higher order TM modes, transverse electric TE modes, transverse electromagnetic TEM modes, or even hybrid modes may yield interesting results. However, to explore these electric modes we would need to introduce the electric vector potential. This

potential is the analog of the magnetic vector potential and has a similar basic wave equation given by

$$\nabla^2 \mathbf{F} + \beta^2 = - \varepsilon \mathbf{M}. \tag{122}$$

The solution to this equation follows from the duality theorem, not to be confused with wave-particle duality, where variables in two equations that occupy the same position are known as dual quantities, and the solution for one of the quantities can be formed by identical exchange of symbols from the other. From here, we can easily expand our previous efforts to cover many alternative planar configurations.

Expanding our solution from the planar geometry the next logical geometries would be cylindrical and spherical geometries. We could possibly foresee a configuration similar to that of a coaxial cable with two superconducting regions separated by a thin insulating region as shown in Figure 24.
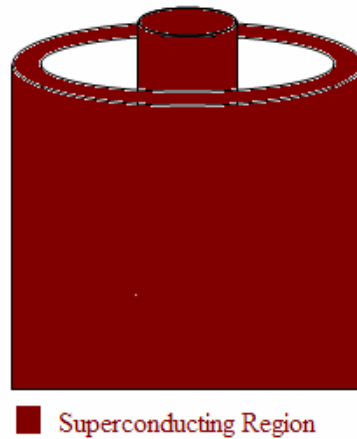

■ Superconducting Region

Figure 24. Coaxial configuration: Two superconducting regions separated by an insulating region.

It may even be interesting to look at the spherically symmetric configuration of two concentric hemispheres. In each of these symmetric geometries we can also attempt to look at the different modes of propagation in a similar manner as we discussed for the planar case.

5.3 Additional Parameters

When we developed our superconducting transmission line formulism we assumed some parameters to be negligible and neglected some of the dependencies of other parameters when we looked at the physical nature of the electromagnetic fields of the structure. There may be some value, in order to obtain highly accurate solutions, to add in other parameters to achieve our goal. In this section we will briefly highlight some of the parameters, which may add to the physical accuracy of our solutions.

The first quantity, which we pointed out before in our solution method to the superconducting transmission line, is the electric potential Φ. This quantity is given by

$$\Phi(x) = \frac{1}{4\pi\varepsilon} \int \frac{\rho(x')}{|x-x'|} d^3x'. \tag{123}$$

We see from the above equation that the electric potential will exist when we have a net charge. In our solution to the superconducting transmission line problem, we assumed no free charge. However, it is likely that a net charge could build up in our device. In this case we would need to add a term using the electric potential as a correction to our original solution. The electric potential will not affect the magnetic field that we calculated, but the equation for the electric field becomes

$$E = -\nabla\Phi - \frac{\partial \mathbf{A}}{\partial t}. \tag{124}$$

In addition to neglecting the free charge in the system under consideration, we also made the simplification that the permeability and permittivity were constant valued, and even further we assumed that they were real quantities. However, the permittivity is notably frequency dependent and begins to have a major impact as we go to higher and higher frequencies. The complex dielectric quantity is then given by [Dressel and Grüner (2002)]

$$\hat{\varepsilon} = \varepsilon_1(\omega) + i\frac{4\pi\sigma_1(\omega)}{\omega}. \tag{125}$$

Here, ε_1 is the real permittivity, σ_1 is the conductivity, and ω is the frequency. We note again that the real permittivity and the conductivity are both frequency dependent as well. This now gives us three "layers" of frequency dependence. Where do we end? Other parameters are also frequency dependent, temperature dependent, pressure dependent, etc. Furthermore there are properties intrinsic to different superconductors such as type 1, type 2, and high temperature superconductors that have been neglected. At some point we must step back and look at the problem we are trying to accomplish. Looking at all of the relations and properties that exist for transmission lines, coupling conditions, and general behavior of all kinds of solids, we see one clear property. Every case is different in some way. We cannot come up with one ultimate formula that will govern all the "real world" properties of every single configuration that nature allows. In order to accurately model a specific system, we must take into account the properties of that specific system. To this end, the best solution may be to combine experimental data of specific materials with solid state and electrodynamic theory in order to form a unique solution for a given system.

APPENDIX A. MATLAB GRAPHING SCRIPTS

In order to simulate the graphics in section 3.1.1 for the electromagnetic fields propagating in the superconducting transmission line, a short script written in MATLAB was utilized in order to handle the 3-dimensional graphics. MATLAB lends itself well to multidimensional analysis and graphics because of its multitude of predefined matrix functions and its ability to handle large and multidimensional arrays efficiently. While MATLAB was used in order to compute the electromagnetic field values, Origin graphical software was used to graph the results.

In addition to the 3-D electromagnetic field graphics shown earlier, short movie files were also created in order to view the dynamic changing of the electromagnetic field values with time. These movies could not be presented here, but are a part of the oral dissertation and can easily be recreated using the sample script shown below. Below then is a sample MATLAB script used to compute the electromagnetic fields in the insulating region. This script both saves files for plotting in Origin as well as creates an AVI file in MATLAB that can be viewed with any compatible AVI player such as Windows Media Player.

```
%%%Electromagnetic field simulator for the fields in the insulating
%%%region of a superconducting transmission line

%Ignore all warnings and clear all variables
warning off;
clear all;

%Initialize constants
w = 100e9; %rad/s
kx = 100;  %1/m
kz = 348; %1/m
c=3e8; %m/s

%Set x and z dimensions for movie axes
```

```
xdim=-40e-5:.25e-5:40e-5;
zdim=-15e-3:.25e-3:15e-3;

%initialize movie image counter
l=1;

%begin time loop
for i=0:.1:10
%initialize row counter
m=0;
    %begin x loop
    for j=-40e-5:.25e-5:40e-5
        %increment row counter
        m=m+1;
        %initialize column counter
        n=0;
        %begin z loop
        for k=-15e-3:.25e-3:15e-3
            %increment column counter
            n=n+1;
            %calculate x-component of Electric field
            Efieldx=c^2*(kz*kx*(exp(kx*j)-exp(-kx*j))*exp(sqrt(-1)*(kz*k-
w*i)));
            %calculate z-component of Electric field
            Efieldz=c^2*(kx^2*(exp(kx*j)+exp(-kx*j))*exp(sqrt(-1)*(kz*k-
w*i)));
            %calculate magnitude of electric field
            Efield(m,n) = sqrt(Efieldx^2+Efieldz^2);
            %calculate Magnetic field
            Bfield(m,n)=-kx*(exp(kx*j)-exp(-kx*j))*exp(sqrt(-1)*(kz*k-
w*i));
        %end z loop
        end
    %end x loop
    end
        %String Concactinate time counter
        istr = strcat(num2str(i),' (s)');
        %Start a new figure for Efield movie image
        figure(4)
        %Clear previous figure
        clf;
        %Plot 3-d countours of Electric field using 100 contours
        contour3(zdim,xdim,Efield,100)
        %Hold the current figure to plot over
        hold on
        %Set axis dimensions and ticklength
        axis([-15e-3,15e-3,-40e-5,40e-5])
        set(gca,'TickLength',[.025,.025])
        %Label x and y axes and enter current time as title
        xlabel('Distance (m)')
        ylabel('Distance (m)')
        title(istr)
        %Add frame to movie
        M(:,l)=getframe;
        %Turn off figure hold
```

```matlab
            hold off

            %Start new figure for Bfield movie image
            figure(6)
            %Similar setup as for Efield
            clf;
            contour3(zdim,xdim,Bfield,100)
            hold on
            axis([-15e-3,15e-3,-40e-5,40e-5])
            set(gca,'TickLength',[.025,.025])
            xlabel('Distance (m)')
            ylabel('Distance (m)')
            title(istr)
            %Add frame to Bfield movie
            D(:,l)=getframe;
            hold off
            %Increment movie frame
            l=l+1;

            %Use if statements to save files at time = 1,2,3,and 4 seconds
            if i==1
             save Efield1.dat Efield -ascii -tabs
             save Bfield1.dat Bfield -ascii -tabs
            elseif i==2
             save Efield2.dat Efield -ascii -tabs
             save Bfield2.dat Bfield -ascii -tabs
            elseif i==3
             save Efield3.dat Efield -ascii -tabs
             save Bfield3.dat Bfield -ascii -tabs
            elseif i==4
             save Efield4.dat Efield -ascii -tabs
             save Bfield4.dat Bfield -ascii -tabs
            end

    %end time loop
    end

    %Initialize file and store Electric field movie
    aviobj = avifile('EfieldVid','compression','indeo5', 'FPS', 10);
    %Add frames to Electric field movie
    aviobj = addframe(aviobj,M);

    %Initialize file and store Magnetic field movie
    aviobj = avifile('BfieldVid','compression','indeo5', 'FPS', 10);
    aviobj = addframe(aviobj,D);
    %Close AVI files so they are no longer writeable and can be viewed.
    aviobj = close(aviobj);
```

APPENDIX B. MATHEMATICA COMPUTATIONS

In order to calculate the numerical results shown in section 3.2.1., Mathematica's numerical derivative (ND) solver was used. The ND solver enables graphical representation of complex differential equations, including transcendental equations such as the Sine-Gordon equation.   This ability then makes the ND solver the perfect choice for solving this particular equation. The first two equations solved in the example Mathematica notebook shown below are for the general form of the linear approximation and non approximated forms of the Sine-Gordon equation over a time period of 15 seconds. The third and fourth graphical representations are for the specific form of the Sine-Gordon equation relating to the coupling between superconductors in a weak-link Josephson junction. These are the figures we saw in section 3.2.1 for the time period of 0 to 0.01 seconds. Below is a sample Mathematica notebook used to solve different forms of the Sine-Gordon equation under unique boundary conditions.

Linear Approximation to the Sine-Gordon equation

```
NDSolve[{D[y[x, t], t, t] == D[y[x, t], x, x] + y[x, t]
  y[x, 0] == Exp[-x^2], Derivative[0, 1][y][x, 0] == 0
  y[-10, t] == y[10, t]}, y, {x, -10, 10},
 {t, 0, 15}]
{{y -> InterpolatingFunction[{{-10, 10.}, {0., 15.}},
Plot3D[Evaluate[y[x, t] /. First[%]], {x, -10, 10},
 {t, 0, 10}, PlotPoints -> 30]
```
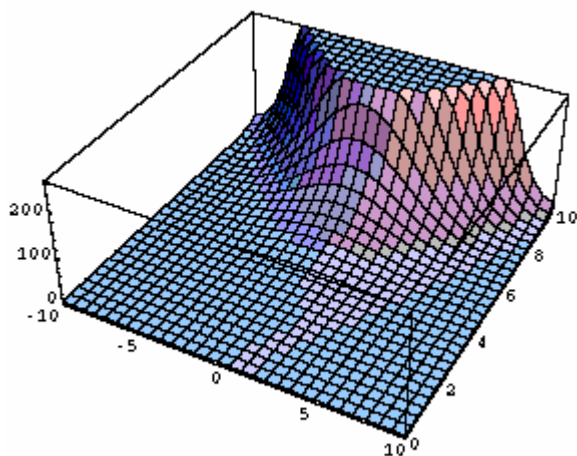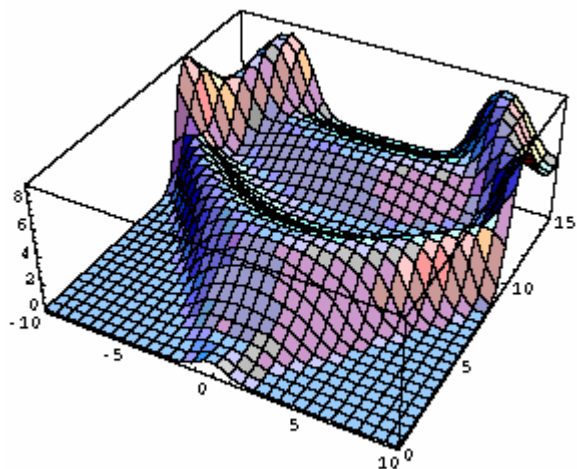
Non-linear Solution to the Sine-Gordon equation

```
NDSolve[{D[y[x, t], t, t] ==
    D[y[x, t], x, x] + Sin[y[x, t]], y[x, 0] == Exp[-x^2
  Derivative[0, 1][y][x, 0] == 0, y[-10, t] == y[10, t]
 y, {x, -10, 10}, {t, 0, 15}]
{{y → InterpolatingFunction[{{-10, 10.}, {0., 15.}}, ·
Plot3D[Evaluate[y[x, t] /. First[%]], {x, -10, 10},
 {t, 0, 15}, PlotPoints -> 30]
```
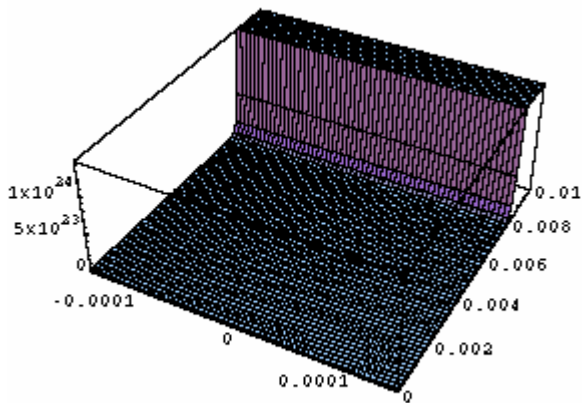
Non-linear solution using values of ω=c/20 and λ_J=150e-6m

```
NDSolve[
  {D[y[x, t], t, t] == D[y[x, t], x, x] * 20 / (3 * 10^8)
     y[x, t] / (150 * 10^-6)^2,
   y[x, 0] == Exp[-x^2], Derivative[0, 1][y][x, 0] == 0
   y[-150 * 10^-6, t] == y[150 * 10^-6, t]}, y,
  {x, -150 * 10^-6, 150 * 10^-6}, {t, 0, .01}]
{{y → InterpolatingFunction[
     {{-0.00015, 0.00015}, {0., 0.01}}, <>]}}
Plot3D[Evaluate[y[x, t] /. First[%]],
  {x, -150 * 10^-6, 150 * 10^-6}, {t, 0, .01},
  PlotPoints -> 60]
```



```
NDSolve[
  {D[y[x, t], t, t] == D[y[x, t], x, x] * 20 / (3 * 10^8)
     Sin[y[x, t]] / (150 * 10^-6)^2,
   y[x, 0] == Exp[-x^2], Derivative[0, 1][y][x, 0] == 0
   y[-150 * 10^-6, t] == y[150 * 10^-6, t]}, y,
  {x, -150 * 10^-6, 150 * 10^-6}, {t, 0, .01}]
{{y → InterpolatingFunction[
     {{-0.00015, 0.00015}, {0., 0.01}}, <>]}}
Plot3D[Evaluate[y[x, t] /. First[%]],
  {x, -150 * 10^-6, 150 * 10^-6}, {t, 0, .01},
  PlotPoints -> 60]
```
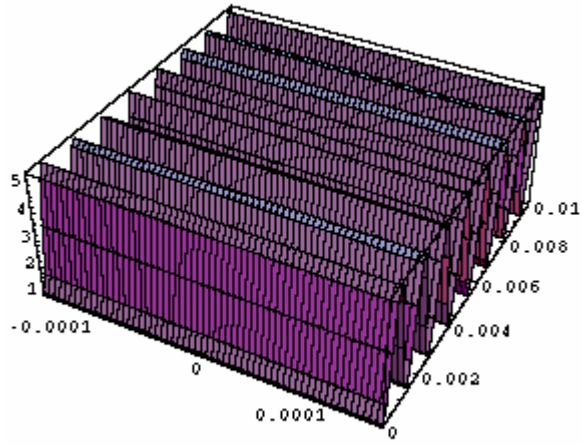
APPENDIX C. MATLAB: FINITE DIFFERENCE METHOD

As we discussed earlier in Section 3.2.2., we decided to use a Matlab script in order to solve for the electromagnetic fields in our Josephson junction using the current from the AC Josephson effect. In this section we described the setup of this problem, so here we will simply present the actual Matlab scripts written and some results.

The following is the initial script used to numerically solve for the magnetic vector potential of a Josephson junction.

```matlab
warning off;
clear all;
%Modified 5/15/07
%Calculate A for a Josephson Junction
%initialize array
Nx=200;
A=zeros(Nx);
%Spacing if used
dx=.0000001;
dt=.0000001;
%frequency Hz
f=10;
%current density, since J(0)=5, J=5cos(wt)
J=5;
mu=.0000000001;

Rmin=0;
w = 1;
count=1;
while (count < 1000)&(max(A)<10000)
    Rmin=0;
    point=0;
    if mod(count,10)==0
        fprintf('%g \n',count)
    end
for j=2:(Nx-1)
    for i=2:(Nx-1)
    if (i<75 | i>125)
        x(j,i)=5;

        if j==2
            A(i,j-1)=0;
        elseif j==Nx-1
            A(i,j+1)=0;
        end
        R = A(i-1,j)+A(i+1,j)-A(i,j-1)-A(i,j+1)+mu*dx*dt*A(i,j);
```

```
        Rmin = Rmin+abs(R);
        point=point+1;
        A(i,j) = A(i,j)+(w/4)*R;
    elseif (i>74 & i<126)
        x(j,i)=0;
    if j==2
        A(i,j-1)=0;
    elseif j==Nx-1
        A(i,j+1)=0;
    end
     R = A(i-1,j)+A(i+1,j)-A(i,j-1)-A(i,j+1)-mu*dx*dt*J*cos(f*j);;
        Rmin = Rmin+abs(R);
        point=point+1;
        A(i,j) = A(i,j)+(w/4)*R;

    end
  end
end

count=count+1;
Rmin=Rmin/point;
end
save Junction.dat x -ascii -tabs
save Josephson.dat A -ascii -tabs

contourf(A)
```

Earlier we saw the geometry of the problem was entered correctly and below we see the result for the magnetic vector potential obtained using this script. In the figure below we see that we have a single, very large, negative region occurring inside one of the superconducting regions. It is interesting that we do not see a symmetric result about the center of the z-component of the junction, since the junction and its initial conditions are symmetric about this axis. If we were to have calculated the electromagnetic fields from this vector potential, they would also be present and oscillatory in the same region as we see the magnetic vector potential. This result is not intuitive nor in line with the results we obtained before. Therefore, we consider this an incorrect result. The debugging of this solution and the extension of this solution to calculate the electromagnetic fields, will be the focus of future directions.
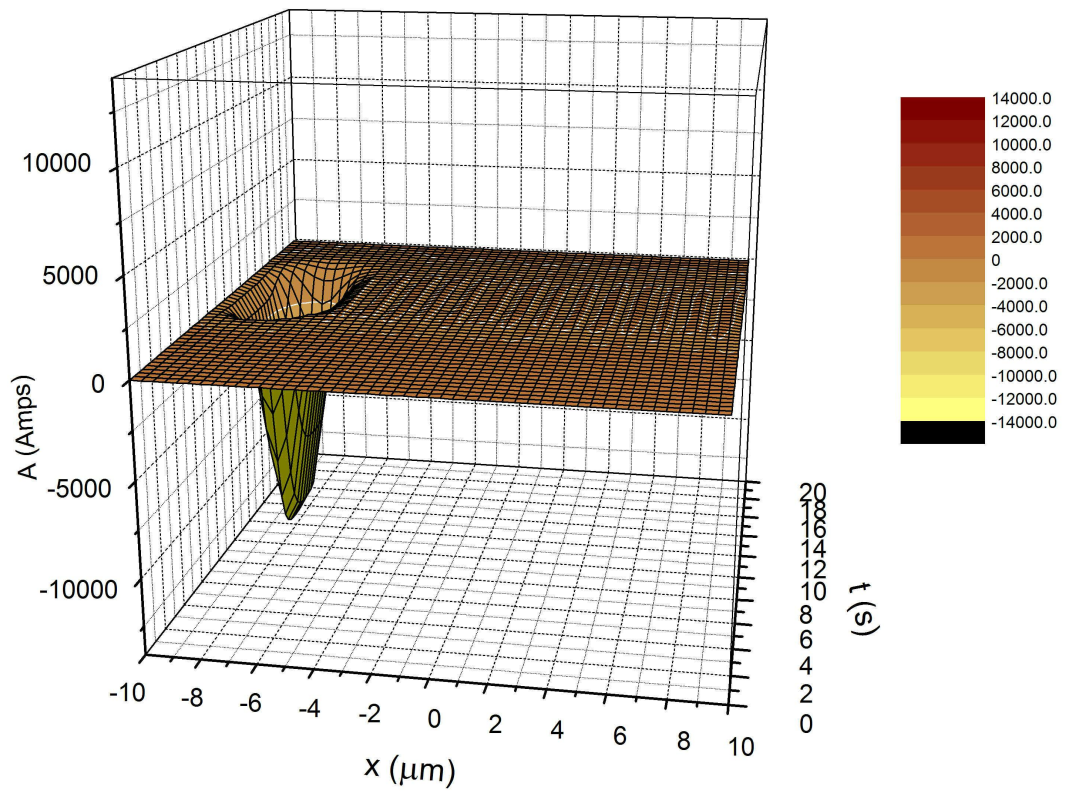
BIBLIOGRAPHY

Anderson, N. E., Mina, M., and Babaei Brojeny, A. A. (2006). On the Utilization of Magnetic Vector Potential for a Description of a Superconducting Transmission Line. *IEEE Trans. Appl. Supercond*. 16(3):1913-1917.

Ashcroft, N. W. and Mermin, N. D. (1976). *Solid State Physics*. Australia: Thomas Learning, Inc.

Balanis, C. A. (1989). *Advanced Engineering Electromagnetics*. New York: John Wiley & Sons.

Barone, A. and Paternò, G. (1982). *Physics and Applications of the Josephson Effect*. New York: John Wiley & Sons.

Clarke, J., Goubau, W., and Ketchen, M. (1975). A reliable DC squid made with tunnel junctions. *IEEE Trans. Magn.*, 11(2):724-727.

Dressel, M. and Grüner, G. (2002). *Electrodynamics of Solids*. Cambridge: Cambridge University Press.

Faoro, L., Siewert, J., and Fazio, R. (2003). Non-Abelian Holonomies, Charge Pumping, and Quantum Computation with Josephson Junctions. *Phys. Rev. Lett.,* 90(2):028301-1 – 028301-4.

Ginzburg, V.L. and Andryushin, E. A. (2004). *Superconductivity*. Singapore: World Scientific.

Gorter, C. J. and Casimir, H. B. G. (1934). On Supraconductivity. *Physica*, 1:306-320.

Jackson, J.D. (1999). *Classical Electrodynamics*. New York: John Wiley & Sons Inc.

Josephson, B. D. (1962). Possible new effects in superconductive tunneling. *Phys. Rev. Lett.*, 1:251-253.

Josephson, B. D. (1964). Coupled Superconductors. *Rev. Mod. Phys.*, 36:216-220.

Josephson, B. D. (1974). The Discovery of Tunneling Supercurrents. *Science*, 184(4136):527-530.

Kittel, C. (1996). *Introduction to Solid State Physics*. New York: John Wiley & Sons, Inc.

London, F. and London, H. (1935). The Electromagnetic Equations of the Supraconductor. *Proc. Roy. Soc.*, 149:71-88.

Parker, W. H., Taylor, B. N., and Langenberg, D. N. (1967). Measurement of 2e / h Using the ac Josephson Effect and its Implications for Quantum Electrodynamics. *Phys. Rev. Lett.*, 18(8):287-291.

Pippard, A. B. (1947). The surface impedance of superconductors and normal metals at high frequencies. I. Resistance of superconducting tin and mercury at 1200Mcyc./sec. *Proc. Roy. Soc.*, A191:370-384.

Pippard, A. B. (1947). The surface impedance of superconductors and normal metals at high frequencies. II. The anomalous skin effect in normal metals. *Proc. Roy. Soc.*, A191:385-399.

Pippard, A. B. (1947). The surface impedance of superconductors and normal metals at high frequencies. III. The relation between impedance and superconducting penetration depth. *Proc. Roy. Soc.*, A191:399-415.

Pond, J. M., Weaver, P., and Kaufman, I. (1989). Propagation Characteristics of Inductively-Coupled Superconducting Microstrip. *IEEE MTT-S Digest*, 451-454.

Sadiku, M. (2001). *Numerical Techniques*. New York, CRC Press, Inc.

Shapiro, S. (1963). Josephson currents in superconducting tunneling: The effect of microwaves and other observations. *Phys. Rev. Lett.*, 11:80-82.

Suzuki, K., Hayashi, K., Murphy, A., Fujimoto, M., Yoshikawa, S., Yamaguchi, K., and Enomoto, Y. (1994). Y-Ba-Cu-O Mixer Antenna Array at 23 GHz. *IEEE MTT-S Digest*, 1001–1004.

Swihart, J. C. (1960). Field Solution for a Thin-Film Superconducting Strip Transmission Line. *J. Appl. Phys.*, 32(3):461-469.

Wu, P. H., Wang, H. B., Chen, J., and Yamashita, T. (2002). Propagation of an electromagnetic wave in a stack of superconducting layers. *Supercond. Sci. Technol.* 15:364-369.

ACKNOWLEDGEMENTS

There have been many people over the years that have motivated, encourage, and inspired me in my education and in life. They have helped me build a strong foundation and find joy in both work and life. I would first like to thank my wife Cassie. She has helped me through the sleepless nights and been there through all my successes and all my failures always encouraging me. Without her, it is very likely that this paper would never have been written. Of course I would like to thank my advisor Mani. I remember my first class with Mani. He had such a joy teaching and explained electromagnetism so beautifully that I had to learn more about the subject. Throughout my career, Mani has always been such an inspiration and I am glad that he has believed in me all throughout this process. I would also like to thank my committee members Robert Weber and Alex Travesset. I appreciate the time they have taken and their accommodativeness. I have fond memories of both of their courses and have used the things I have learned in both my research and at my job. I would also like to take the opportunity to thank Paul Canfield, who I first began my research career with over 8 years ago. It was because of Paul that I found a true enjoyment in the work that I did and decided to pursue graduate research. Finally, I would like to thank my parents. They have supported me in all my endeavors throughout my life and continue to do so to this very day. I am truly thankful for everything they have done.